UCRL-17484

University of California

Ernest O. Lawrence Radiation Laboratory

PHYSICAL-REGION DISCONTINUITY EQUATIONS FOR MANY-PARTICLE SCATTERING AMPLITUDES. I

Berkeley, California

Submitted to
Journal of Mathematical Physics

UCRL-17484
Preprint

UNIVERSITY OF CALIFORNIA

Lawrence Radiation Laboratory
Berkeley, California

AEC Contract No. W-7405-eng-48

PHYSICAL-REGION DISCONTINUITY EQUATIONS FOR MANY-PARTICLE SCATTERING AMPLITUDES. I

Joseph Coster and Henry P. Stapp

April 13, 1967

PHYSICAL-REGION DISCONTINUITY EQUATIONS FOR MANY-PARTICLE SCATTERING AMPLITUDES. I*

Joseph Coster and Henry P. Stapp

Lawrence Radiation Laboratory
University of California
Berkeley, California

April 13, 1967

ABSTRACT

The discontinuity equations are derived for all singularities of multiparticle scattering functions that enter the portion of the physical region lying below the four-particle threshold. These equations, which are the precise statements of the Cutkosky formulas, are calculated directly from the unitarity equations. The only analyticity properties used are those obtained from the S-matrix macroscopic causality condition. That is, the scattering functions are taken to be analytic in the physical region except on positive-α Landau surfaces, around which they continue in accordance with the well-defined plus-iϵ rule.

The problem of finding discontinuity formulas has been examined earlier in the S-matrix framework by Gunson,[2] Stapp,[3] and Olive.[4] Their approach has been essentially to verify, within certain approximations, the consistency of certain conjectured discontinuity formulas. Certain normal-threshold discontinuity formulas have been derived by Hwa using crossing, and working to lowest order.[5]

More recently Landshoff and Olive[6] have derived the discontinuity across the singularity of the triangle diagram of the $3 \to 3$ amplitude in the physical region, and their method has been applied by others[7-10] to singularities associated with various other diagrams. The method of Landshoff and Olive is, however, quite complicated. It requires a detailed investigation of specific features of Landau curves, an examination of the properties of certain integrals, and a tracing of paths of continuation, and it depends on delicate cancellations of various terms. Also it requires a complete enumeration of the "generation" and "regeneration" mechanisms of the singularity, and this is not easily obtained except in the simplest cases. Finally each singularity is a separate problem.

In the present paper we develop an alternative method for calculating the discontinuities of the (connected part) physical-region scattering amplitude M^+. This function has singularities only on positive-α Landau surfaces, and it can be continued past these in accordance with a well-defined plus-iϵ rule.[11,12] The discontinuities around these singularities will be obtained in this paper directly from the unitarity equations through manipulations that bring these equations into a form that displays explicitly the appropriate discontinuity function. Specifically, a unitarity equation is converted, using unitarity, into the form

$$M^+ = T(D) + R(D) \,, \tag{1.1}$$

where $T(D)$ vanishes on one side (called the unphysical side) of the positive-α Landau surface $\mathcal{M}^+[D]$ associated with the Landau diagram D, and $R(D)$ is known to have a minus-$i\epsilon$ continuation around $\mathcal{M}^+[D]$. That $R(D)$ has a minus-$i\epsilon$ continuation around $\mathcal{M}^+[D]$ means that the function $R(D)$ is carried into itself by a continuation around $\mathcal{M}^+[D]$ in the sense opposite to the sense that carries M^+ into itself. Since $T(D)$ vanishes on the unphysical side of $\mathcal{M}^+[D]$, the function $R(D)$ constitutes an explicit expression for the continuation of M^+ around $\mathcal{M}^+[D]$ in the minus-$i\epsilon$ sense, and (1.1) displays $T(D)$ as the discontinuity of M^+ around $\mathcal{M}^+[D]$.

In this first article a bubble-diagram notation is set up that facilitates manipulations of the unitarity equations. Various results needed from earlier work[13] concerning the analytic structure of bubble-diagram functions are summarized, and a general theorem fundamental to our approach is proved. The method is then exhibited for the special case of $3 \to 3$ reactions below the four-particle threshold, and we obtain the discontinuity formulas for every physical-region singularity. The results for the $3 \to 2$ and $2 \to 3$ reactions can be obtained from these formulas by regarding an appropriate pair of external lines as a single line.

The results in the $3 \to 3$ case are easily summarized. All the positive-α Landau surfaces below the four-particle threshold are contained in the surfaces corresponding to the set of diagrams shown in Fig. 1 together with those obtained from these diagrams by the procedure explained in the caption. [The other possible Landau diagrams, some of which are shown in Fig. 2, give no additional surfaces and hence can be ignored.] The discontinuity of M^+ around the Landau surface $\mathcal{M}^+[D]$ for any one of these diagrams D is expressed as an integral over a product of a set of functions consisting of one physical scattering amplitude (the connected part of the S matrix, which is diagrammatically represented by a plus bubble) for each vertex V_n of D and one function F_{nm} for each pair of vertices (V_n, V_m). If there is no elementary line segment L_j directly connecting V_n to V_m, then F_{nm} is unity. If exactly one L_j directly connects V_n to V_m, then F_{nm} is $2\pi\, \delta(p_j^2 - \mu_j^2)\, \theta(p_j^0)$. If two or three lines L_j directly connect V_n to V_m, then F_{nm} is a function defined in terms of physical scattering amplitudes by a Fredholm integral equation.

The rules giving the discontinuity can be expressed in the diagrammatic form

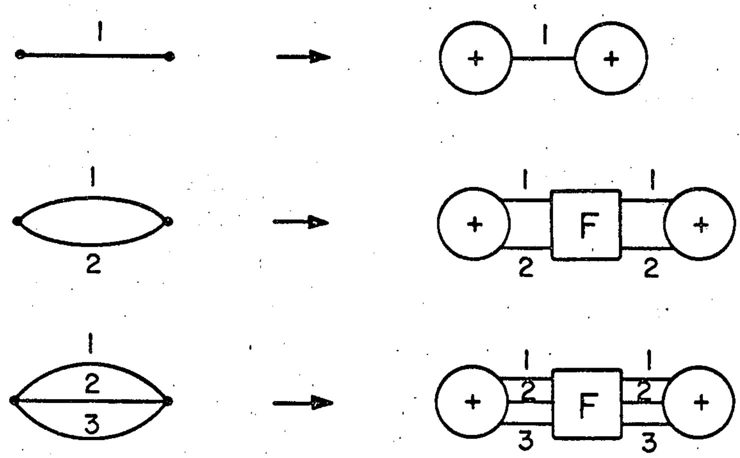

(1.2)

where the left-hand diagrams denote the part of a Landau diagram D that connects V_n to V_m, with all the lines not directly connecting V_n to V_m suppressed. The right-hand diagrams denote the corresponding part of the bubble-diagram function that gives the discontinuity across $\mathcal{M}^+[D]$, with the F box representing F_{nm}. Thus, for example, the discontinuity of M^+ across $\mathcal{M}^+[D]$, where

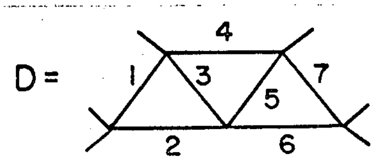

(1.3)

is represented by

T (D) = 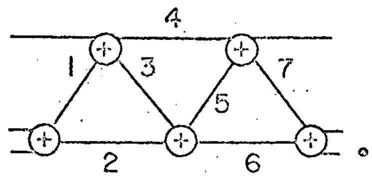

(1.4)

But if the diagram has two-particle closed loops, as does for example

D′ = 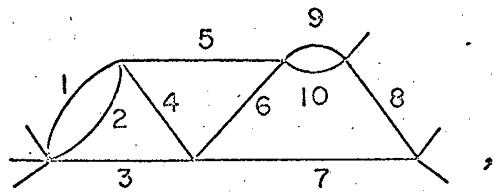

(1.5)

then, according to (1.2), an F box is added for each of these. Thus the discontinuity of M^{+} around the Landau surface corresponding to (1.5) is given by

T(D′)= 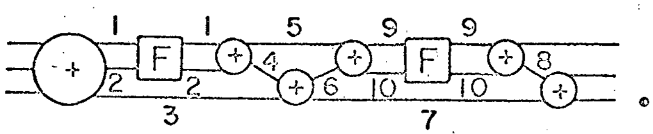

(1.6)

We also obtain formulas for the discontinuities across various classes of singularities. For example, the discontinuity of M^{+} across the class of Landau surfaces that correspond to all diagrams of the form

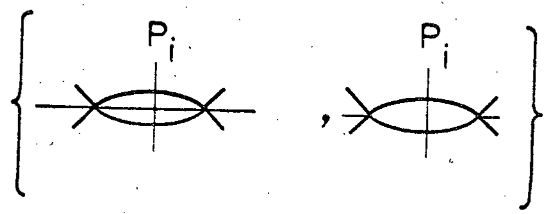

(1.7)

plus all diagrams that can be contracted to a diagram of this class is given by

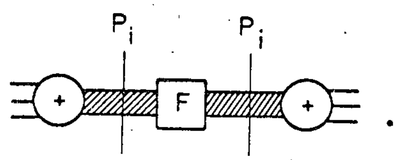

(1.8)

Here the P_i bar restricts the sets of particles represented by the lines it intersects to sets having a sum of rest masses greater than a given mass M_i . A similar result is valid for all diagrams that can be contracted to a diagram of the class

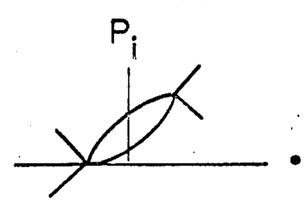

(1.9)

The results described above are derived strictly from the physical-region unitarity equations. They provide a complete solution of the problem of physical-region discontinuities below the four-particle threshold. If one admits also the so-called extended unitarity equations, then it can be shown that the functions F_{nm} convert the scattering functions upon which they operate to their values on other sheets.

The present work deals only with the singularities lying in the physical region. One ultimately wants to have discontinuity formulas also for singularities lying outside the physical region, but the evident initial step is to establish the results first in the physical region, where the unitarity equations apply. On the basis of earlier work[11] it is assumed that the physical-region singularities are confined to the union of the positive-α Landau surfaces, and that the physical continuation around these singularities follows the so-called plus-$i\epsilon$ rules. The existence of the unphysical continuations via minus-$i\epsilon$ rules is proved by using Fredholm theory, apart from possible zeros of the Fredholm denominator.

It is possible that the positive-α Landau surfaces corresponding to two different Landau diagrams are identical. Indeed, if two Landau diagrams are "equivalent", then their Landau surfaces are certainly identical. [Equivalent diagrams are diagrams having the same set of vertices and the same set of masses μ_{nm}. The mass μ_{nm} is defined, in the positive-α case, to be the sum of the rest masses of the set of particles γ_{nm} associated with the set of lines Γ_{nm} that directly connect vertex V_n to vertex V_m.] It is assumed in the present work that the positive-α Landau surfaces corresponding to basic inequivalent diagrams are nonidentical. The diagrams of Fig. 1 and those obtained from them by the procedure of the caption are all the $3\to3$ basic diagrams. [Generally, a basic diagram is one such that the α's are uniquely defined at some point on the positive-α Landau surfaces. The diagrams shown in Fig. 2 are not basic.] This assumption allows us to consider separately the discontinuities associated with different sets of equivalent basic diagrams.

It is possible for a positive-α surface to coincide with a Landau surface associated with α's of mixed sign.[14] A second assumption used in the present work is that there is no cancellation between mixed-α singularities and positive-α singularities. That is, it is assumed that in the unitarity equations, and equations arising from them, the singularities associated with positive-α Landau surfaces will cancel among themselves, as will the singularities associated with the mixed-α diagrams, even though these singularities may happen to occur at the same point. This seems reasonable: Since singularities in the physical region can occur only on positive-α surfaces, it would be unnatural for singularities associated with mixed-α surfaces to contribute to the physical-region discontinuities, even though a mixed-α surface might happen to coincide with a positive-α surface. This assumption allows us effectively to ignore the singularities associated with the mixed-α surfaces.

The validity of the assumptions described in the preceding two paragraphs really should be proved, but this is not attempted here.

II. BUBBLE DIAGRAMS AND LANDAU DIAGRAMS

The basic quantities in this discussion are bubble-diagram functions. These functions are functions of scattering functions that can be represented by bubble diagrams.

A <u>bubble diagram</u> B is a collection of leftward-directed line segments L_j and signed circles called bubbles. Each bubble has at least one line issuing from it and at least one line terminating on it. The bubbles are partially ordered by the requirement that a bubble on which a line terminates stands left of the bubble from which this line issues. A line of B that issues from some bubble of B and also terminates on some bubble of B is called an internal line of B. The other lines of B are called external.

A circle with a plus sign inside represents the connected part of the S matrix for the process obtained by associating initial particles with lines that terminate on the bubble and final particles with lines that issue from the bubble. A circle with a minus sign inside represents the complex conjugate of the connected part of the S matrix for the transpose (initial $\leftrightarrow$ final) of that process. That is, the leftward-directed lines that terminate on a minus bubble are associated with final particles, and the leftward-directed lines issuing from the bubble are associated with initial particles.

Spin variables will be ignored.[15] Then each line L_j is associated with a variable (p_j, t_j), where t_j is an index specifying a type of particle (electron, proton, positron, etc.), the mass of which is $\mu_j \equiv \mu(t_j)$, and p_j is a physical momentum-energy vector satisfying $p_j^2 = \mu_j^2$ and $p_j^0 > 0$.

The bubble diagram B represents a corresponding function $M^B(K';K'')$, which is just the product of the functions represented by the bubbles of B, with the understanding that there is a sum over repeated indices (variables) of these functions. In particular, for each internal line L_j of B there is a sum over all particle types t_j. And for each value of t_j there is an integration over all physical values of the corresponding momentum vectors p_j. Thus, each internal line L_j of a bubble diagram corresponds to a factor

$$\sum_{t_j} \int \frac{d^4 p_j}{(2\pi)^4} \quad 2\pi \quad \theta(p_j^0)\, \delta[p_j^2 - \mu^2(t_j)] \,, \tag{2.1}$$

where a covariant volume element has been chosen. The integration is restricted so that topologically equivalent contributions are counted only once, as is discussed in Appendix A.

Occasionally we shall wish to restrict the sum over t_j associated with internal lines to a sum over particles having a given rest mass. Then the line L_j will be labeled by an integer, which is regarded as specifying a particular value of the rest mass.

The argument $(K';K'')$ of $M^B(K';K'')$ is the set of variables associated with the external lines of B. The lines that issue from bubbles of B are associated in a one-to-one fashion with the variables of the set $K' = (p_1', t_1', \cdots, p_n', t_n')$, and the lines that terminate on bubbles of B are associated in a one-to-one fashion with the variables of the set $K'' = (p_1'', t_1'', \cdots, p_m'', t_m'')$. These two sets of lines are also called the outgoing and incoming lines of B respectively.

Bose statistics is assumed throughout. Then the cluster decomposition of the S matrix is expressed by the equation[16]

$$S(K';K'') = \sum_{B \in B_0^+(K';K'')} M^B(K';K'') . \qquad (2.2)$$

Here $B_0^+(K';K'')$ is the set consisting of all bubble diagrams that have only plus bubbles, have no internal lines, and have external lines specified by $(K';K'')$. That is, the sum is over all different ways of connecting the specified set of external lines to columns of plus bubbles. Only topologically different diagrams are regarded as different; reorderings of lines on a given bubble, or reorderings of the bubbles do not give additional terms (see Appendix A).

The function $S(K';K'')$ is represented by a box with a plus sign inside. A box with a minus sign inside represents the complex conjugate for the transpose of the process. Thus an example of (2.2) is the equation

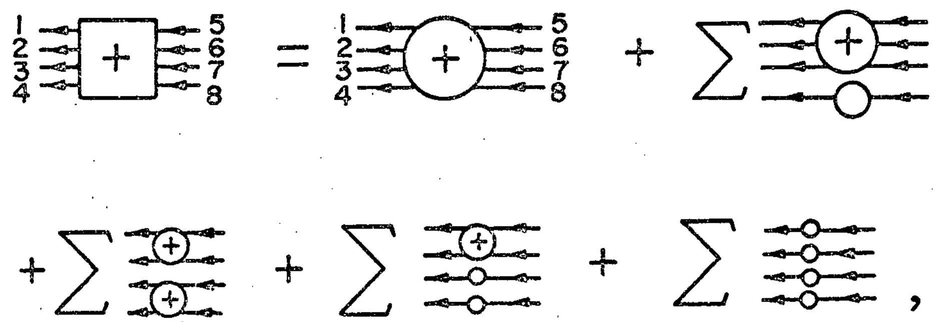

(2.3)

where the sums are over all topologically different ways of connecting the specified set of external lines to bubbles having the indicated numbers of incoming and outgoing lines. Some bubble diagrams always vanish by virtue of conservation laws and mass constraints, and these have been omitted. For example, each nontrivial bubble must connect to at least two incoming and two outgoing lines by virtue of the stability conditions on the physical masses. Trivial bubbles are bubbles from which just one line issues and upon which just one line terminates. The function corresponding to a trivial bubble is defined to be the inverse of (2.1),

$$\frac{(2\pi)^4\ \delta^4(p_r' - p_s'')\ \delta(t_r' - t_s'')}{2\pi\ \delta(p_r'^2 - \mu_r^2)\ \theta(p_r'^0)} \equiv \delta(p_r',\ t_r'\ ;\ p_s'',\ t_s''), \qquad (2.4)$$

where $\delta(a - b) = \delta_{ab}$ for discrete indices. Since (2.4) holds for all trivial bubbles, the signs in these bubbles can be omitted. Often the trivial bubbles themselves will be omitted.

The connected part of the S matrix is denoted by

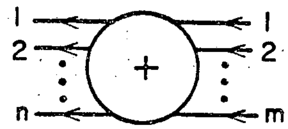

$$\equiv M^{+}(K';\,K'') \equiv M^{+}_{nm} \quad . \qquad (2.5)$$

More generally, the function represented by a bubble with the symbol σ inside is denoted by $M^{\sigma}(K';K'') = M_{nm}^{\sigma}$.

Unitarity is written in box notation as

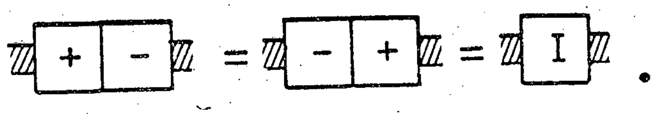

(2.6)

The external lines appropriate to the process in question are represented by shaded strips. There is a sum over all possible numbers of lines crossing the interface of the rectangles. Sometimes these lines are indicated by writing the left side of Eq. (2.6) as

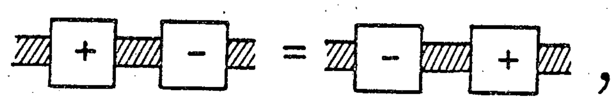

(2.7)

where the shaded strip between the boxes represents the sum over all possible numbers of lines. The right side of (2.6) is zero unless m is equal to n, in which case it is given by

$$\delta(K';K'') = \delta(K'';K')$$

$$= \sum_{\alpha} \prod_{i=1}^{n} \delta(p'_i,\ t'_i;\ p''_{\alpha i},\ t''_{\alpha i}), \qquad (2.8)$$

where the α are the $n!$ permutations on n objects. The last term in (2.3) is the bubble-diagram representation of I for the case $n = 4$.

We often need to subtract from the S matrix the identity, the connected part of the S matrix, or both. The remainders are denoted by special symbols:

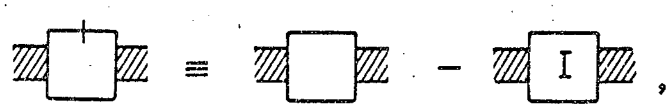

(2.9)

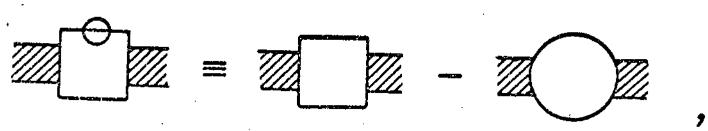

(2.10)

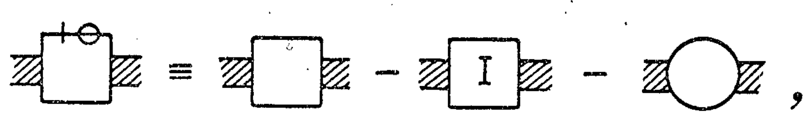

(2.11)

where a common label inside the boxes and bubbles of each equation has been suppressed.

It was shown in Ref. 13 that all singularities of bubble-diagram functions are associated with Landau diagrams.[17] A Landau diagram D is a set of directed line segments L_j and a set of vertices V_n. Each vertex contains end points of three or more lines L_j, and no vertex contains both end points of any one line. Denoting the leading and trailing end points of the line segment L_j by the symbols L_j^+ and L_j^-, respectively, one can characterize the diagram D by the set of numbers ϵ_{jn} defined by

$$\epsilon_{jn} = 1 \qquad \text{if } L_j^+ \subset V_n ,$$

$$\epsilon_{jn} = -1 \qquad \text{if } L_j^- \subset V_n ,$$

or

$$\epsilon_{jn} = 0 \qquad \text{otherwise.}$$

Each line L_j of D is associated with a particle of type t_j and mass μ_j. If particles of type t_j carry a_j units of an additively conserved quantum number "a", then the conditions

$$\sum_j a_j \epsilon_{jn} = 0 \qquad \text{(all } n) \tag{2.12}$$

are required of D .

The lines L_j of D are characterized as being incoming, outgoing, or internal according to the following rules:

L_j is incoming if $\epsilon_{jn} \geqslant 0$ for all n,

L_j is outgoing if $\epsilon_{jn} \leqslant 0$ for all n,

L_j is internal otherwise.

The incoming and outgoing lines of D are called external lines of D. A line that is both incoming and outgoing is called an unscattered line.

A connected Landau diagram is an arcwise-connected Landau diagram. A trivial Landau diagram is a connected Landau diagram with no internal lines.[18]

For each Landau diagram D there is corresponding Landau surface $\mathfrak{M}[D]$. The surface $\mathfrak{M}[D]$ is the set of variables (p_j, t_j) associated with the external lines of D via associations

$$L_j \leftrightarrow (p_j, t_j, \alpha_j) \tag{2.13}$$

that satisfy the (loop) equations

$$\sum_j \alpha_j p_j n_{jf} = 0, \quad \text{(all } f) \tag{2.14}$$

the mass constraints

$$p_j^2 = \mu_j^2, \quad \text{(all } j) \tag{2.15}$$

and the conservation laws (2.12). A particular case of (2.12) is the momentum - energy conservation law

$$\sum_j p_j \epsilon_{jn} = 0. \quad \text{(all } n) \tag{2.16}$$

In Eq. (2.14) n_{jf} is the algebraic number of times the Feynman loop f passes along line L_j in the positive sense, and the α_j associated with each internal line L_j is a nonzero number. The α_j associated with the external L_j play no role, and can be set equal to zero. Each p_j is a real energy - momentum vector with $p_j^o > 0$. The part of $\mathfrak{M}[D]$ that can be realized with all α's positive is denoted by $\mathfrak{M}^+[D]$.

A connection between Landau diagrams and bubble diagrams is set up using the following terminology. A Landau diagram D corresponding to a bubble b is a D with its external lines in one-to-one correspondence with the lines of b . The incoming lines of D are to correspond to the lines terminating on b, and the outgoing lines of D are to correspond to the lines issuing from b. The internal lines of a D corresponding to a bubble b will be said to lie inside b.

A $D' \subset B$ is a Landau diagram D' that can be constructed by replacing each nontrivial bubble b of B by a corresponding connected diagram D_c^b, which might be simply a trivial point vertex V^b. This D_c^b is required to be such that $\mathfrak{M}^+[D_c^b]$ is nonempty. Lines containing only trivial bubbles are replaced by lines containing no vertices.

A contraction $D \supset D'$ of a Landau diagram D' is a Landau diagram D that can be obtained by shrinking to points certain of the internal lines L_i of D', and then removing all those lines L_j of the resulting diagram for which L_j^+ and L_j^- coincide.

The diagram D' is considered a trivial contraction of itself.

A $D \supset \subset B$ is a D such that for some $D' \subset B$, D is a $D \supset D'$. The phrase B supports D means that D is a $D \supset \subset B$. Thus, for example, the bubble diagram B of (1.4) supports the Landau diagram D of (1.3). This terminology is used in the next section to describe the locations of the singularities of bubble-diagram functions.

III. LANDAU SINGULARITIES, STRUCTURE THEOREMS FOR BUBBLE DIAGRAMS, AND THE $i\epsilon$ RULE

In this section we summarize some pertinent results obtained earlier regarding the location and nature of singularities of bubble-diagram functions.

According to the First Structure Theorem of Ref. 13, the singularities of $M^B(K';K'')$ [divided by $(2\pi)^4 \delta^4 (\Sigma p_j' - \Sigma p_j'')$] for any connected B are confined to the closure of the union over nontrivial $D \supset\subset B$ of the Landau surfaces $\mathfrak{M}[D]$.[17]

A concrete representation for the surface $\mathfrak{M}[D]$ is now described.[19]

The geometric significance of the loop equations is that the set of momentum-energy vectors

$$\Delta_j \equiv \alpha_j p_j \tag{3.1}$$

fit together to form a momentum-energy space diagram $\bar{D}$ that is topologically equivalent to the diagram D. That is, the directed internal line segment L_j of D leading from a vertex m to a vertex n (i.e., $\epsilon_{jm} = -1$, $\epsilon_{jn} = 1$) is mapped to the four-vector

$$\Delta_j = \omega_n - \omega_m = \sum_r \epsilon_{jr} \omega_r \tag{3.2}$$

of $\bar{D}$, where ω_r is the four-vector from some arbitrary origin to the vertex V_r of $\bar{D}$. The allowed values of the ω_n are those values such that each vector $(\omega_n - \omega_m) \epsilon_{jn}|\epsilon_{jm}| = \alpha_j p_j \epsilon_{jn}|\epsilon_{jm}|$ is positive timelike, negative timelike, or zero, according to whether $\alpha_j \epsilon_{jn}|\epsilon_{jm}|$ is positive, negative, or zero. This is just the requirement that p_j be positive timelike. A typical diagram $\bar{D}$ is shown in Fig. 3.

Each diagram $\bar{D}$ corresponds to exactly one point on $\mathfrak{M}[D]$, and each point of $\mathfrak{M}[D]$ corresponds to at least one diagram $\bar{D}$. The correspondence is given by the mapping function

$$q_n(\omega) = \sum_{m \neq n} \frac{\omega_n - \omega_m}{|\omega_n - \omega_m|} \mu_{nm} , \tag{3.3}$$

where

$$\mu_{nm} = \sum_j \mu_j |\epsilon_{jn} \epsilon_{jm} \alpha_j|/\alpha_j \tag{3.4}$$

and where the denominator is the Lorentz length

$$|\omega_n - \omega_m| \equiv [(\omega_n - \omega_m)(\omega_n - \omega_m)]^{1/2} . \tag{3.5}$$

This length is necessarily positive for $\mu_{nm} \neq 0$, since $\omega_n - \omega_m$ is timelike in this case. The terms where $\mu_{nm} = 0$ do not contribute to (3.3).

The vector q_n occurring in (3.3) is the total outgoing momentum at vertex V_n,

$$q_n = - \sum_{\text{ex } j} p_j \, \epsilon_{jn} , \tag{3.6}$$

where the sum over j runs over the j corresponding to external lines of D. The Landau surface $\mathfrak{M}[D]$ depends on the external p_j only through these combinations q_n. If no external lines are incident on vertex V_n, then q_n is required to vanish. If exactly one external line is incident on V_n then q_n is required to satisfy the corresponding mass constraint.

Equation (3.3) is obtained by first using the conservation law (2.16) to convert (3.6) to a sum over internal lines of D and then using (3.1) and (3.2):

$$\begin{aligned} q_n &= \sum_{\text{int } i} p_i \, \epsilon_{in} = \sum_{\text{int } i} \frac{\Delta_i}{\alpha_i} \epsilon_{in} \\ &= \sum_{\text{int } i} \epsilon_{in} \sum_{m} \epsilon_{im} \omega_m / \alpha_i \\ &= - \sum_{\text{int } i} \sum_{m \neq n} \epsilon_{in} \, \epsilon_{im} (\omega_n - \omega_m)/\alpha_i \\ &= \sum_{\text{int } i} \sum_{m \neq n} |\epsilon_{in} \, \epsilon_{im}| \, (\omega_n - \omega_m)/\alpha_i , \end{aligned} \tag{3.7}$$

where we have observed that for a given internal i only two values of m give a nonzero ϵ_{im}, and that these two ϵ_{im} have opposite signs. From (3.1) and (3.2) one obtains

$$\frac{|\alpha_i|\ \mu_i}{|\omega_n - \omega_m|} = 1, \tag{3.8}$$

which combines with (3.7) to give (3.3):

$$q_n = \sum_{m \neq n} \sum_{\text{int } i} |\epsilon_{im}\, \epsilon_{in}\ \alpha_i| \frac{(\omega_n - \omega_m)\ \mu_i}{|\omega_n - \omega_m|\ \alpha_i}$$

$$= \sum_{m \neq n} \sum_{i} |\epsilon_{im}\, \epsilon_{in}\, \alpha_i| \frac{(\omega_n - \omega_m)\ \mu_i}{|\omega_n - \omega_m|\ \alpha_i} \quad . \tag{3.9}$$

A point $q(\omega)$ of $\mathfrak{M}[D]$ such that the first-order variations $\delta q = (\partial q/\partial \omega)\, \delta\omega$ generate the tangent space to $\mathfrak{M}[D]$ at $q(\omega)$ is called a simple point $q(\omega)$ of $\mathfrak{M}[D]$. If $\mathfrak{M}[D]$ is considered as a surface in $q \equiv \{q_n\}$ space, then the tangent space to $\mathfrak{M}[D]$ at a simple point $q(\omega)$ of $\mathfrak{M}[D]$ lies in the linear manifold defined by

$$q \cdot \omega = q(\omega) \cdot \omega , \tag{3.10}$$

where

$$q \cdot \omega \equiv \sum_{n} q_n \cdot \omega_n \equiv \sum_{n,\mu} q_n^{\ \mu}\ \omega_{n\mu} \equiv \sigma(q,\omega). \tag{3.11}$$

This follows from the fact that, at $\omega' = \omega$,

$$\partial \sigma[q(\omega'),\omega] \ / \ \partial \omega' = 0 \ . \tag{3.12}$$

Equation (3.12) is readily verified by substituting the right side of (3.3) into (3.11) and taking the partial derivative with respect to a component $\omega'_{n\mu}$ of ω'. The vector ω is, in this sense, a normal vector to $\mathfrak{M}[D]$ at a simple point $q(\omega)$ of $\mathfrak{M}[D]$.

The mapping $q(\omega)$ is not one-to-one. All values of ω that are related by changes of the origin or by rescalings of the α_i give the same $q(\omega)$, and are called equivalent. It is convenient to fix the origin by requiring $\sum \omega_n = 0$. Then ω lies in the same manifold as q, which is restricted by $\sum q_n = 0$ due to momentum-energy conservation. The scaling can be fixed up to a single sign by requiring that

$$\sum_{n>m} \sum_i |\omega_m - \omega_n| \, |\epsilon_{in} \; \epsilon_{im}| \equiv \sum_{\text{int } i} |\alpha_i p_i| = 1 .$$

As already mentioned, the First Structure Theorem asserts that the singularities of $M^B(K';K'') \equiv M^B(K)$ for any connected B are confined to the closure of the union over nontrivial $D \supset\subset B$ of the Landau surfaces $\mathfrak{M}[D]$. Let this union be denoted by $\mathfrak{M}^B$. A simple point of $\mathfrak{M}^B$ is a point such that a complete neighborhood of K in $\mathfrak{M}^B$ is generated by an arbitrarily small neighborhood of some unique (up to equivalence) point ω, for some unique nontrivial $D \supset\subset B$. According to the Second Structure Theorem of Ref. 13 such a point cannot actually be a singularity of $M^B(K)$ unless $\bar{D}$ can be realized by taking all $\alpha_i \eta_i \geqslant 0$, where η_i is the sign of the bubble inside which L_i lies, or is zero in case L_i does not lie inside any bubble of B. That is, we can require the α_i of lines L_i of $D \supset\subset B$ that lie in plus (minus) bubbles to be positive (negative), but the α_i of lines of $D \supset\subset B$ that are also lines of the original bubble diagram B are allowed to be either positive or negative.[20]

According to the Third Structure Theorem of Ref. 13 the functions $M^B(K)$ lying on the two sides of the singularity surface at a simple point $\bar{K}$ of $\mathcal{M}^B$ are boundary values of a single function analytic near $\bar{K}$ in the upper-half $\sigma(K;\bar{K}) \equiv \sigma[q(K),\omega(\bar{K})]$ plane, provided at least one line of the corresponding $D \supset\subset B$ lies inside some bubble b of B. The sign of σ is fixed through (3.1) and (3.2) by the requirement $\alpha_i \eta_i \geqslant 0$, which has force only if at least one line L_i of D lies inside some bubble b of B.

In accordance with the Second Structure Theorem we may consider the signs of the α_i to be restricted by the condition $\alpha_i \eta_i \geqslant 0$. Then the singularity at a simple point of $\mathcal{M}^B$ can be classified as either a positive-α, negative-α, or mixed-α singularity, according to whether the various α_i corresponding [via (3.1) and (3.2)] to the singularity are all positive, all negative, or neither all positive or all negative. Thus if B consists of a single plus bubble, then all its singularities are positive-α singularities, but if B consists of a single minus bubble, then all of its singularities are negative-α singularities. The positive-α and negative-α singularity surfaces corresponding to a diagram D both occupy the same position, $\mathcal{M}^+[D]$, but the sign of $\sigma(q,\omega)$ is opposite, and hence the two continuations pass into opposite half planes. A continuation in accordance with the rules for going around a positive-α singularity will be called a continuation according to the plus-$i\epsilon$ rule, whereas a continuation in accordance with the rules for going around a negative-α singularity will be called a continuation according to the minus-$i\epsilon$ rule.

The function $q(K)$ appearing in $\sigma(K;\bar{K}) \equiv \sigma[q(K);\omega(\bar{K})]$ is the expression for the q_n in terms of external vectors given in (3.6). One can also write q as a function of the internal vectors p_i as in (3.7). This gives, again via (3.2) and then (3.1),

$$\begin{aligned} \sigma[q(p_i),\omega] &= \sum_n q_n(p_i)\cdot\omega_n \\ &= \sum_n \sum_{\text{int } i} \epsilon_{in}\, p_i\cdot\omega_n \\ &= \sum_{\text{int } i} p_i\cdot \Delta_i(\omega) \\ &= \sum_{\text{int } i} \alpha_i\, p_i\cdot p_i(\omega)\ . \end{aligned} \tag{3.13}$$

The vector $p_i(\omega)$ is a real positive-energy vector satisfying $p_i(\omega)^2 = \mu_i^2$. Hence the minimum value of $p_i\cdot p_i(\omega)$, when the real vector p_i is restricted by $p_i^2 = \mu_i^2$ and $p_i^0 > 0$, is precisely $\mu_i^2 = p_i(\omega)\cdot p_i(\omega)$. Thus if all the α_j are positive then we have

$$\sigma[q(p_i),\omega] \geq \sigma[q(p_i(\omega)),\omega] \, . \tag{3.14}$$

That is, the function $\sigma[q(p_i),\omega]$ takes its minimum value at $p_i = p_i(\omega)$.

Equation (3.14) has several important consequences. Consider any Landau diagram D. The "physical region" of D is the set of all points in the space of external variables such that there is a set of real p_i associated with the internal lines of D for which the mass constraints (2.15), the energy condition $p_i^0 > 0$, and the conservation laws (2.16) are satisfied. Equation (3.14) says that for any ω corresponding to a point on $\mathfrak{M}^+[D]$ the entire physical region of D, considered as a region in q space, lies on the positive side of the hyperplane $\sigma(q,\omega) = \sigma[q(\omega),\omega]$, except for the point of contact $q = q(\omega)$. This fact was first noticed by Pham.[12] It tells us in particular that the points of $\mathfrak{M}^+[D]$ are necessarily on the boundary of the physical region of D (a result that is not always true on $\mathfrak{M}[D] - \mathfrak{M}^+[D]$) and moreover that $\sigma(q,\omega)$ increases (rather than decreases) as one moves from outside the physical region to inside the physical region at the point $q(\omega)$. It follows from this that the continuation according to the plus-iϵ rule around any positive-α singularity is such that it passes into the upper half plane in any variable z for which $\delta q = (\partial q/\partial z)\, \delta z$ moves the point q from $\mathfrak{M}^+[D]$ into the physical region of D when δz is real and positive. That is, the requirement that $\delta \sigma = \delta q \cdot \omega$

be positive for positive δz implies that $(\partial q/\partial z)\cdot\omega > 0$, which means that for $\mathrm{Im}\,\delta z > 0$ one has

$$\delta\,\mathrm{Im}\,\sigma = \omega\cdot\mathrm{Im}\,\delta q = \omega\cdot(\partial q/\partial z)\,\mathrm{Im}\,\delta z > 0.$$

Thus, the continuation according to the plus-$i\epsilon$ rule always goes into the upper half plane of a variable that is increasing as one moves into the physical region.

The Landau diagram $D \subset B$ obtained by replacing each bubble b of B by a point vertex V^b is denoted by D^B. The function M^B is not generally continuable past the singularity at $\mathcal{M}[D^B]$. Indeed, the above result shows that the function M^B vanishes on one side of $\mathcal{M}^+[D^B]$ but not on the other side. These two sides are called the unphysical and physical sides, respectively. The function M^B evidently has both positive-α and negative-α singularities at $\mathcal{M}^+[D^B]$, since the constraints $\alpha_i\,\eta_i \geqslant 0$ allow for $\bar{D}$ with either all α_i positive or all negative, since all the η_i are zero.

IV. DEVELOPMENT OF THE UNITARITY EQUATION FOR THE $3 \to 3$ SCATTERING AMPLITUDE

Suppose the center-of-mass energy E of the initial (or final) particles is below the 4-particle threshold. Then the connected part of the unitarity equation (2.6) for the $3 \to 3$ amplitude can be written in the form

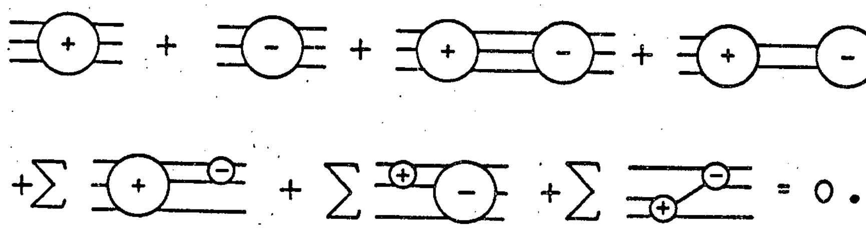

(4.1)

The unmarked summation signs in (4.1) and in the subsequent equations refer to the external lines (incoming and outgoing). Those that will be marked "i" or "f" refer only to incoming or outgoing lines, respectively. These sums are over all topologically different ways of connecting the specified set of external lines to the rest of the bubble diagram. For example, the last term in (4.1) has nine contributions, whereas the fifth term has three:

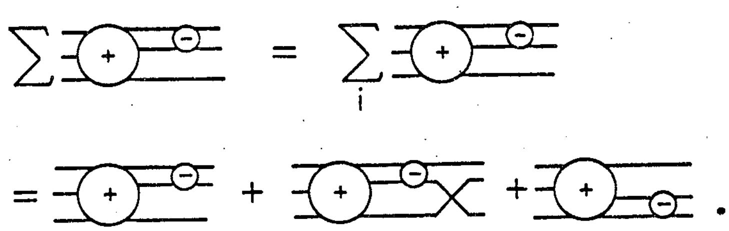

(4.2)

The external lines, reading from top to bottom, represent fixed variables (p_j, t_j), but the internal lines are subject to the summation convention of Sec. II unless it is restricted by explicitly labeling an internal line by an integer. Thus, for instance, we have

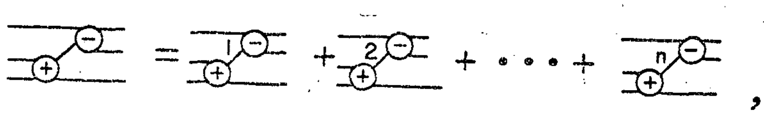

(4.3)

where the number r on an internal line restricts the summation to particles of a fixed mass M_r.

Postmultiplying (4.1) by

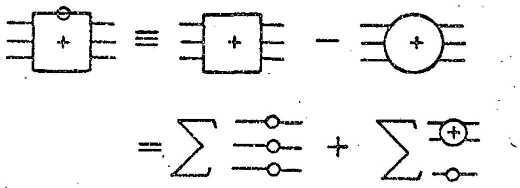

(4.4)

and simplifying by means of two-particle unitarity,

(4.5)

we obtain

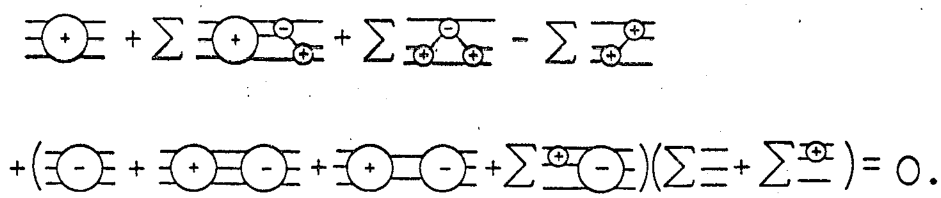

(4.6)

[A detailed discussion of combinatorial questions is given in Appendix A. Our rules are such that the products of functions represented by diagrams such as (4.1) and (4.4) are always represented simply as the sum of the topologically distinct diagrams that can be obtained by combining the diagrams in the natural fashion. By product we mean, of course, matrix product; there is an integration (2.1) over the internal lines.]

Again using (4.5) we may write

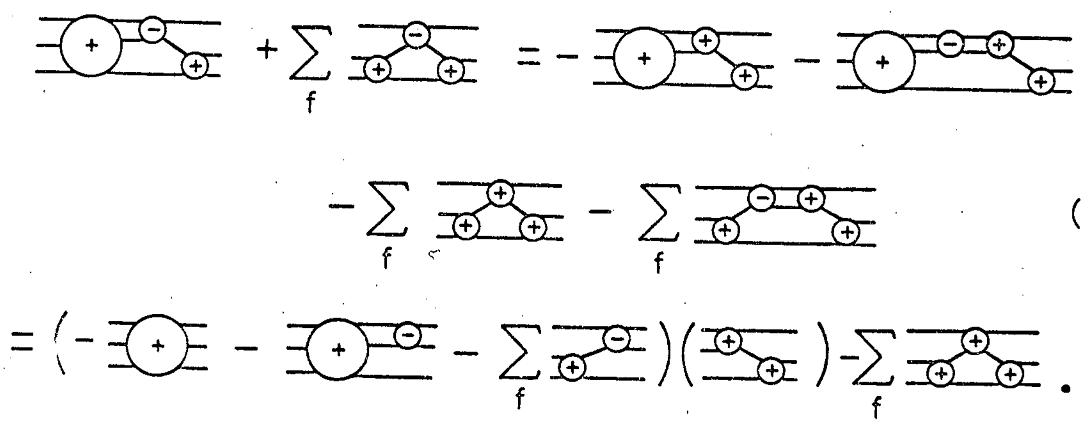

(4.7)

Application of (4.1) to the expression in the left parentheses gives

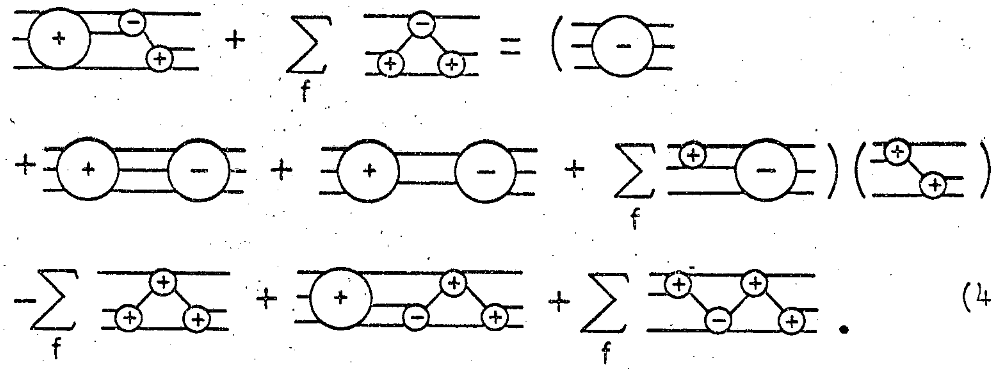

(4.8)

There is an equation similar to (4.8) but with the right plus bubble connected to the upper two lines. Substituting that equation into the last two terms of the right side of (4.8), we obtain

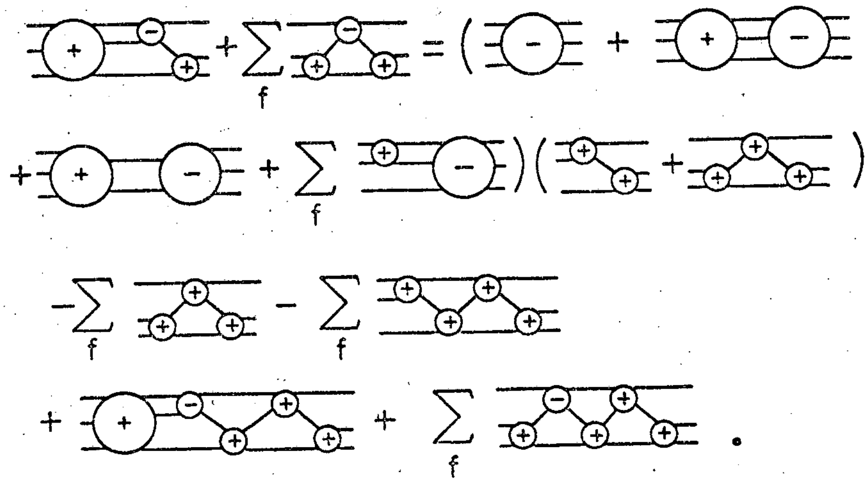

(4.9)

Equation (4.9) can be iterated by substituting the right side of (4.9) into the last two terms of the right side of (4.9). Iterating n times, we end up with the equation

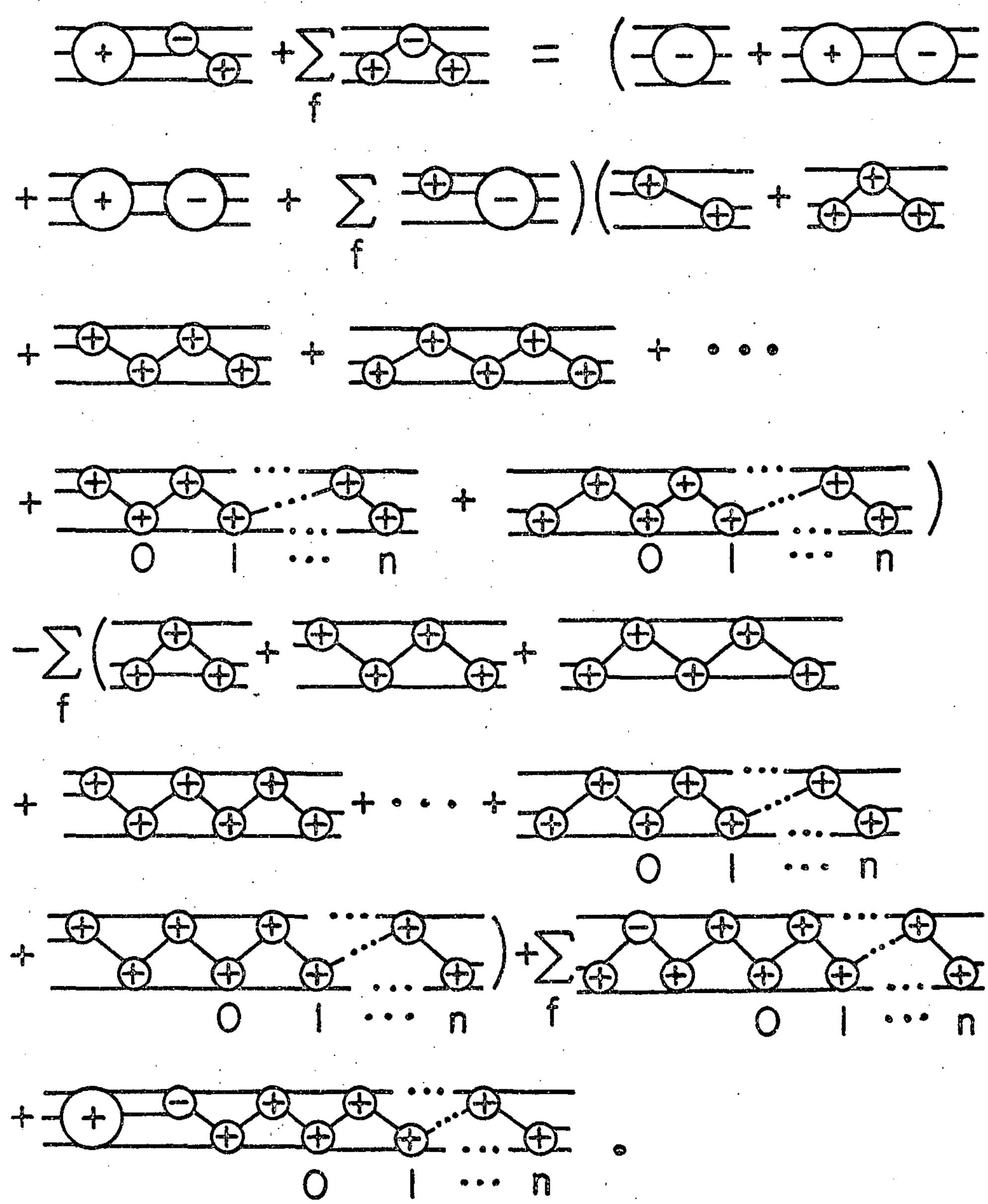

(4.10)

Substituting (4.10) into (4.6) we obtain for any positive integer n

$$M_{33}^{+} + H^{n} + G^{n} + C^{n} + R_{-}^{n} = 0 , \qquad (4.11)$$

where

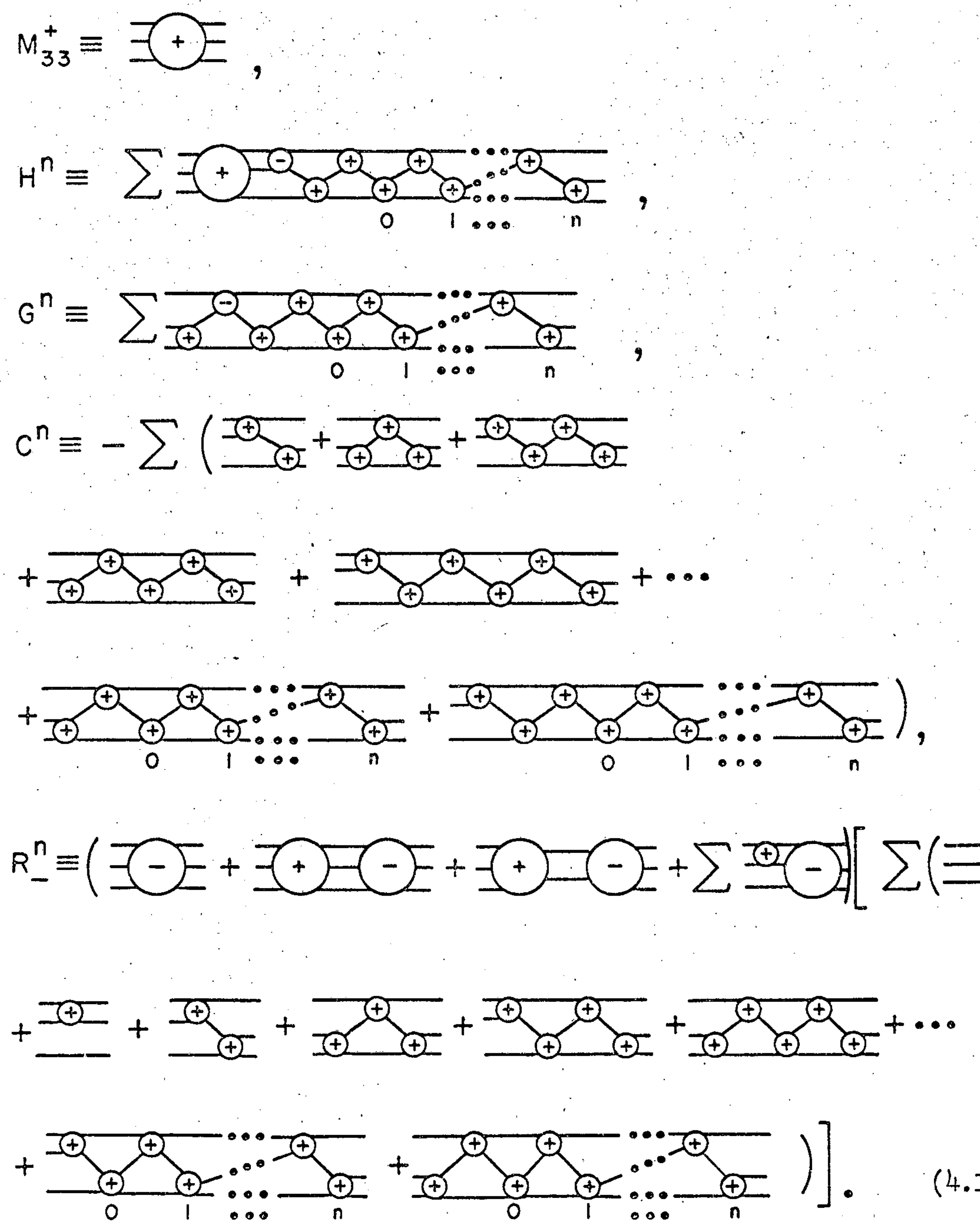

(4.12)

V. DERIVATION OF DISCONTINUITY EQUATIONS

A. Discontinuities Across Singularities Depending on a Cross-Energy

Certain Landau diagrams D are such that every continuous curve within D connecting any incoming line to any outgoing line must pass through one and the same vertex V (see Fig. 4). The Landau surfaces corresponding to such diagrams can depend on the total energy and on the various subenergies, but with a suitable choice of variables they are independent of all cross-energy invariants.[21] Landau surfaces $\mathfrak{M}[D]$ corresponding to diagrams D of this type will be called surfaces of type A. Singularities not lying on surfaces of type A will be called cross-energy singularities. The discontinuity equations for all cross-energy singularities of M^+_{33} can be obtained directly from (4.11) and the structure theorems.

The singularities of the various terms in (4.11) must cancel. Since M^+_{33} is regular at points not lying on $\mathfrak{M}^+$, the singularities of $H^n + G^n + C^n + R^n_-$ corresponding to α's of mixed sign (mixed-α singularities) must cancel among themselves at these points. As discussed in the introduction, we shall assume that this cancellation among mixed-α singularities holds true also at points of $\mathfrak{M}^+$. We also assume that the surfaces $\mathfrak{M}^+[D]$ corresponding to inequivalent basic diagrams D are nonidentical and consider points lying on a single one of these surfaces.

By virtue of the first assumption, we can, in deriving the discontinuities of M^+_{33}, ignore the mixed-α singularities of the various terms in (4.11). According to the First Structure Theorem the singularities of M^B are confined to the union over $\mathcal{M}[D]$ of the nontrivial $D \supset \subset B$. Consider first G^n. [We sometimes use the same symbol to denote both the bubble diagram and its function.] If any one of the diagonal lines of G^n is contracted to give D, then $\mathcal{M}[D]$ is of type A. This is because the only allowed diagrams in the $2 \to 2$ bubbles must have, as a consequence of the stability and the positive- (or negative-) α requirements, both incoming lines terminating on a common vertex and both outgoing lines issuing from a common vertex. On the other hand, if any of the horizontal lines of G^n is contracted, then the two diagonal lines lying above or below this horizontal line must also be contracted, as a consequence of the Landau loop equations and the positive- (or negative-) α requirement. Thus, all the positive- (or negative-) α cross-energy singularities of G^n correspond to diagrams D in which none of the (explicitly appearing) lines of G^n are contracted. But for sufficiently large n, the $\mathcal{M}^+[D]$ for such a D does not enter the region below the four-particle threshold. [This was proved in Ref. 22 by proving that for sufficiently large n the classical point-particle multiscattering process pictured by D is dynamically impossible.]

A similar argument shows that H^n can have no positive- (or negative-) α cross-energy singularities, provided n is taken sufficiently large.

The diagrams $D \supset \subset B$ for $M^B \epsilon R^n_-$ have, for the Landau diagrams D_c^b corresponding to the $3 \to 3$ or the $3 \to 2$ minus bubbles, either a point vertex V^b or a nontrivial diagram with internal lines. In the former case $\mathfrak{M}[D]$ is of type A. In the latter case, the fact that D contains some line that lies inside a minus bubble means that the α_i of at least one line of $\bar{D}$ must be negative. Since all α_i must have the same sign, this universal sign must be negative. Thus, the σ of the Third Structure Theorem that defines the continuation past this singularity of R^n_- is the negative of the σ associated with the same singularity of M^+_{33}. That is, the continuation around this singularity of R^n_- follows the minus-iϵ rule.

We may now derive the discontinuity of M^+_{33} across the singularity corresponding to the Landau surface $\mathfrak{M}^+[D]$ associated with any diagram D that may be formed by contracting to points the bubbles of a bubble diagram B_D having labeled lines that represents a contribution to C^n. For example, the diagram

D = 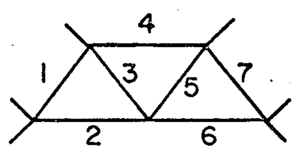

(5.1a)

corresponds to the contribution to C_n

M^{B_D} = 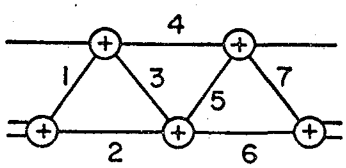

. (5.1b)

According to the remarks at the end of Section III the term $T(D) \equiv M^{B_D}$ is a threshold term present in (4.11) for points on the physical side of $\mathcal{M}^+[D]$, but absent on the unphysical side. If one takes Eq. (4.11) on the unphysical side and continues around the singularity in accordance with the minus-$i\epsilon$ rule, then R^n_- is continued into the same function R^n_- that occurs on the physical side of the $\mathcal{M}^+[D]$, by virtue of the Third Structure Theorem. However, the function M^+_{33} is continued to its value underneath the cut (or underneath the pole). This continuation is denoted by $M^+_{33}(D^-)$. The remaining terms are not singular at the point in question and are therefore continued into the same functions that occur on the physical side of $\mathcal{M}^+[D]$. Thus, the difference between the continuation of (4.11) from the unphysical side and (4.11) evaluated on the physical side of $\mathcal{M}^+[D]$ gives simply

$$\Delta_D M^+_{33} \equiv M^+_{33} - M^+_{33}(D^-) = M^{B_D} \equiv T(D). \qquad (5.2)$$

That is, the discontinuity around the singularity surface $\mathcal{M}^+[D]$ is just M^{B_D}.

The essential point in this method is that the expansion of M^+_{33} be such that all positive-α contributions to the singularity in question that are not in M^+_{33} itself are contained in a "threshold term", which is a term that contributes on only one side of the singularity surface in question. This is the key point of this paper.

The surfaces $\mathcal{M}^+[D]$ considered above are not the only positive-α Landau surfaces that are not of type A. Other D's can be obtained by inserting some internal structure in some of the plus bubbles of a bubble diagram corresponding to a term of C^n. The stability and positive-α requirements, together with the total-energy limitation, allow the insertions only of chains of the form

D_c^b = 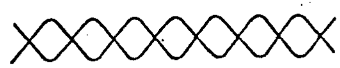 , (5.3)

where the Landau equations require that the sum of the masses of each link of the chain be the same. Since the Landau surfaces corresponding to such a chain do not depend on the number $n \geqslant 1$ of closed loops, we can, without loss of generality, limit the chains to a single closed loop. Then, we obtain, for instance, the Landau diagram

D_1 = 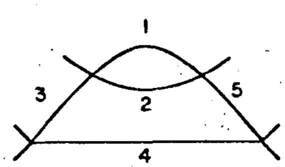

. (5.4)

In order to obtain the discontinuity equation for the cut starting at $\mathcal{M}^+[D_1]$, and also for later use, we now cast the unitarity equation into a form where only the scattering amplitude itself and a threshold term have a positive-α singularity corresponding to a given normal threshold. Let us introduce the decomposition

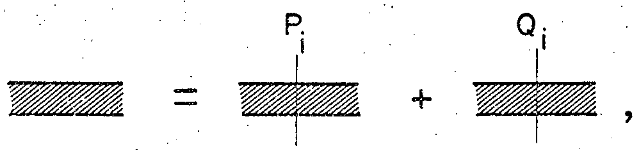

(5.5)

where the P_i (or Q_i) bar restricts each of the sets of particles corresponding to the lines intersected by the bar to a set having a sum of rest masses greater than or equal to (or smaller than) a given mass M_i. Using (2.9) and (5.5) we can write (2.6) in the form

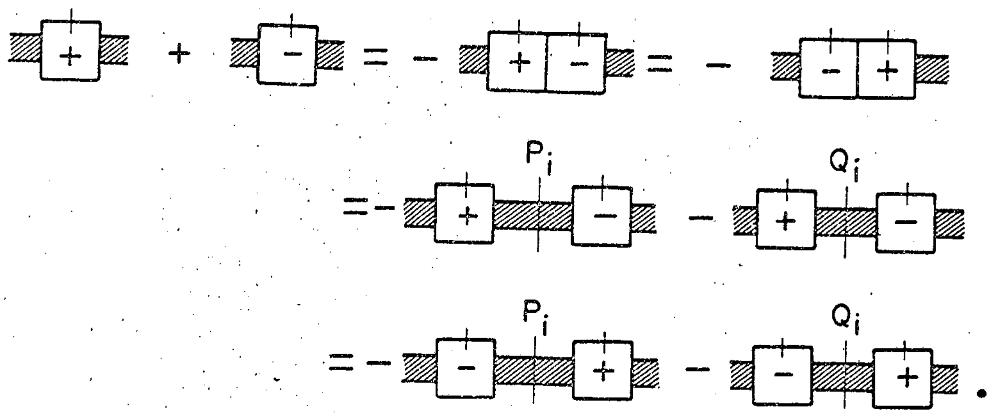

(5.6)

Instead of the bars we often use the more compact notation exhibited in

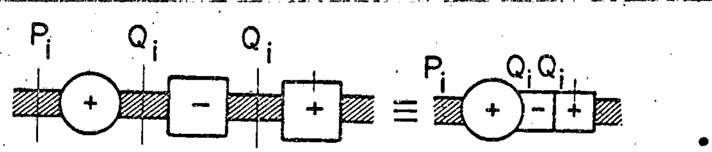

(5.7)

Denoting the center-of-mass energy of the incoming particles by E, we see that only the second term on the right side of (5.6) contributes below $E = M_i$. We define the <u>i box</u> by the equation[23]

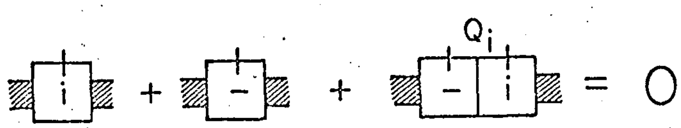

(5.8)

for both $E < M_i$ and $E > M_i$. [In this equation, and those that follow, E is assumed to be below the four-particle threshold.] An i box is related to i bubbles in the same way as a plus box is related to plus bubbles. Thus, we have

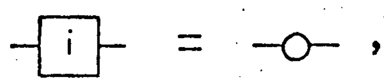

(5.9a)

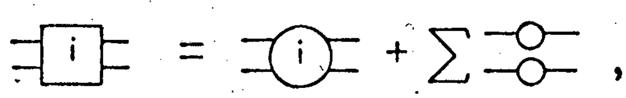

(5.9b)

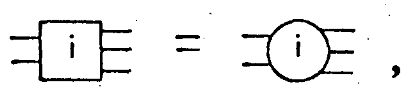

(5.9c)

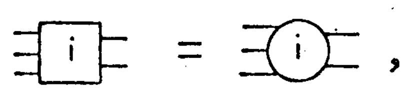

(5.9d)

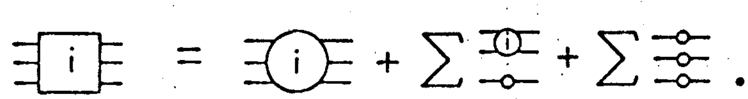

(5.9e)

The functions represented by the i bubbles will be denoted by $M^i(K';K")$. These functions depend on the mass M_i associated with Q_i. The $2 \to 2$ i bubble in (5.9e) is defined by the required vanishing of the various disconnected parts of (5.8). The disconnected part equation

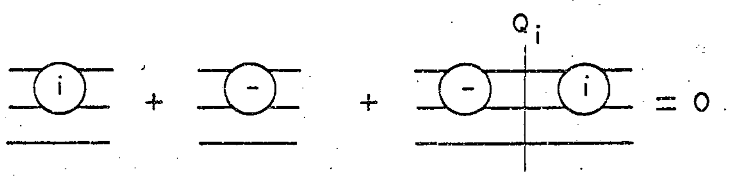

(5.10)

is equivalent to

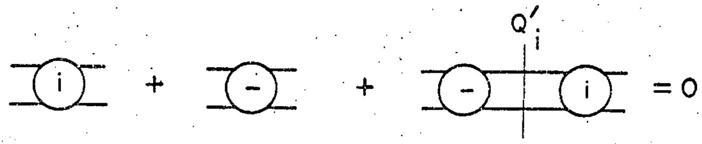

(5.11)

if the mass M'_i associated with the Q'_i of (5.11) is related to the mass M_i associated with the Q_i of (5.10) by $M'_i = M_i - \mu_i$, where μ_i is the rest mass of the spectator particle in (5.10).

It is shown in Appendix B that (5.8) can be solved for $M^i(K';K")$ by using Fredholm theory and that $M^i(K';K")$ has a minus $i\epsilon$ continuation past the normal threshold singularity at $E = M_i$. This result follows formally directly from the iterative solution

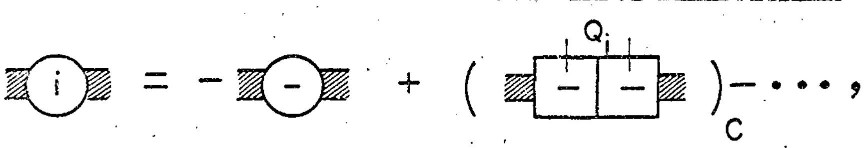

(5.12)

where the subscript C indicates the connected part of the expression in parentheses. For example, in the $2 \to 2$ case (5.12) becomes

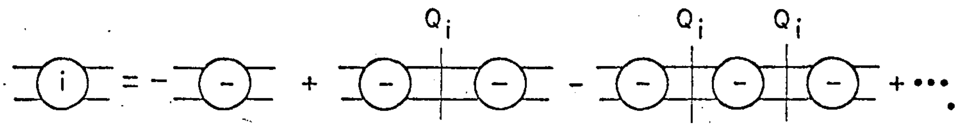

(5.13)

Let B be any term on the right side of (5.13) and consider the normal threshold corresponding to the Landau diagram D

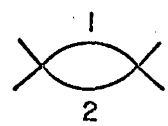

, (5.14)

where $M_i = \mu_1 + \mu_2$. Because of the Q_i projections any $D \supset\subset B$ must have negative α's associated with its lines. Then the Third Structure Theorem prescribes a minus-iϵ continuation past the singularity of M^B at $\mathfrak{M}^+[D]$. Thus each term on the right of (5.13) must follow a minus-iϵ rule past this normal threshold.

Similarly, it follows from (5.12) that M^i_{33} has a minus-iϵ continuation past the normal thresholds corresponding to the diagrams

(5.15)

where we put M_i equal to $\mu_1 + \mu_2 + \mu_3$ or $\mu_1 + \mu_2$, respectively. These results can be made rigorous by using Fredholm theory in place of (5.12), as is shown in Appendix B.

From (5.6) and (5.8) we obtain[24]

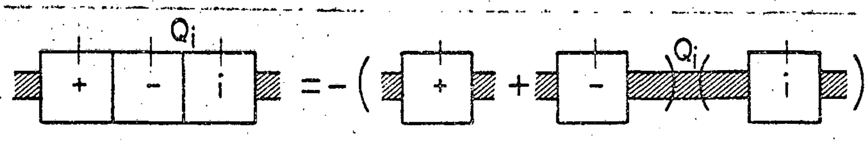

(5.16)

and also

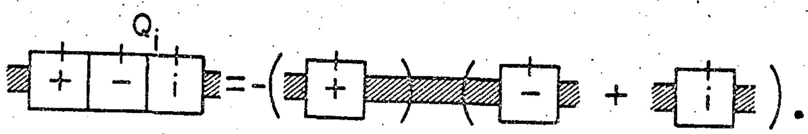

(5.17)

Comparing (5.16) and (5.17) we obtain

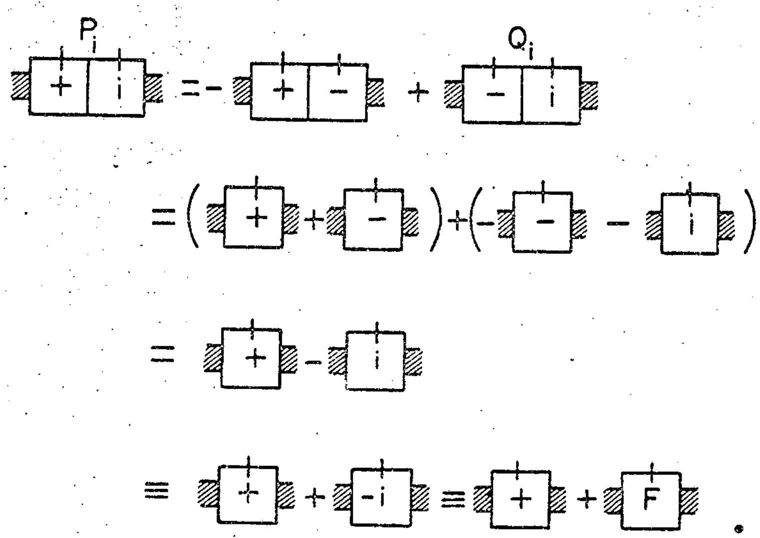

(5.18)

In Appendix C we show that

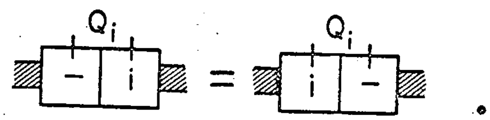

(5.19)

Using (5.19) one obtains also (5.18) with the i box and plus box interchanged on the left side, and hence also

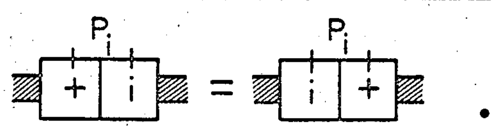

(5.20)

It follows from (5.11) and (5.19), and from (5.18), (5.20), and (2.9), that

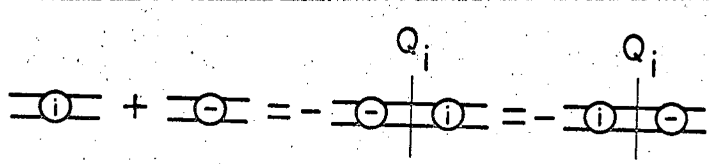

(5.21)

and that

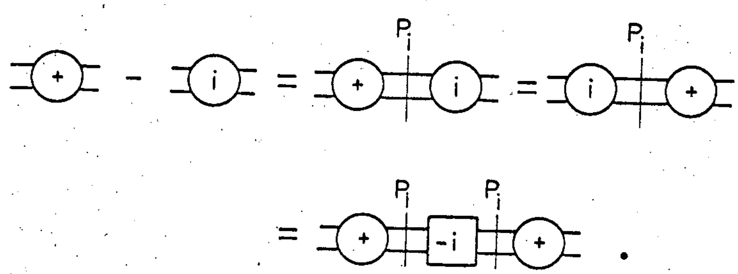

(5.22)

In (5.22) only the first term on the left side and the threshold term on the right side have a positive-α singularity corresponding to the diagram (5.14) where $M_i = \mu_1 + \mu_2$. This shows that M_{22}^i is the continuation of M^+_{22} below this singularity and that the discontinuity is the right side of (5.22).

Returning now to the problem of the discontinuity around $\mathfrak{M}^+[D_1]$, where D_1 is defined in (5.4), we use (5.22) to expand the relevant term T of C^n as follows:

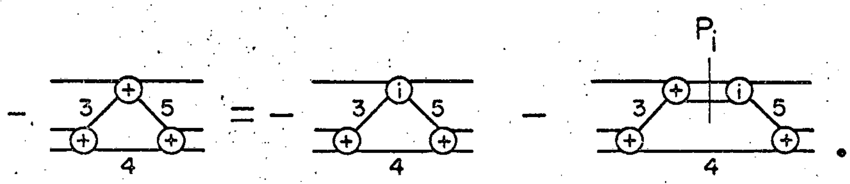

(5.23)

Setting M_i equal to $\mu_1 + \mu_2$, we see that the first term of this expansion has a minus $i\epsilon$ continuation past the surface $\mathfrak{M}^+[D_1]$ for just the same reason that R^n_- does. The second term has its threshold at $\mathfrak{M}^+[D_1]$. Therefore we obtain in the same way as before the discontinuity equation

$$\Delta_{D_1} M^+_{33} = T(D_1), \tag{5.24}$$

where

T (D$_1$) =

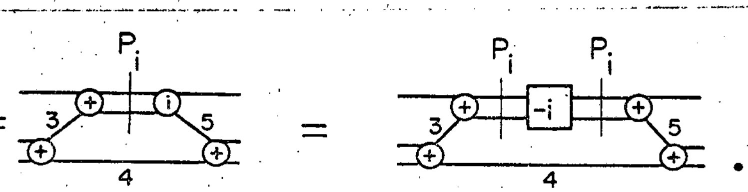

(5.25)

The method given above can be generalized. Any set of inner plus bubbles (that is, plus bubbles not standing at the extreme right or the extreme left of the bubble diagram) of any bubble diagram

T corresponding to a term T of C^n can be replaced by closed loops, while the remaining plus bubbles are contracted to points. The corresponding discontinuity of M_{33}^+ is then given by T with every plus bubble corresponding to a two-particle closed loop replaced by

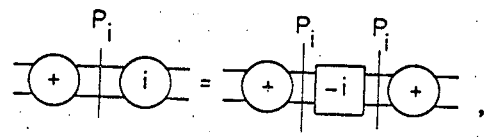

(5.26)

with the index i referring to the sum of the rest masses of the two particles in the two-particle closed loop.

B. Discontinuity Equation for Normal Singularities in a Subenergy

To derive the discontinuity of M_{33}^+ across $\mathfrak{M}^+[D_2]$ where

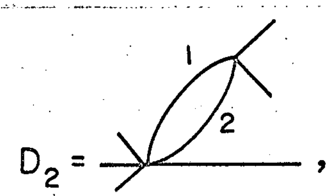

(5.27)

we first write the first and fifth term of (4.1) in the form

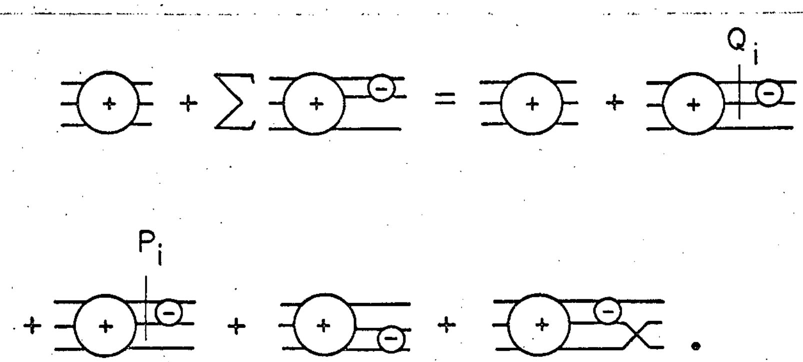

(5.28)

Substituting (5.28) into (4.1), postmultiplying the result by

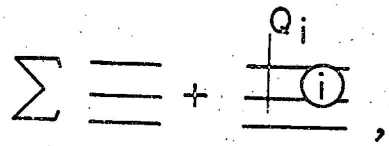

(5.29)

and using (5.21), we obtain

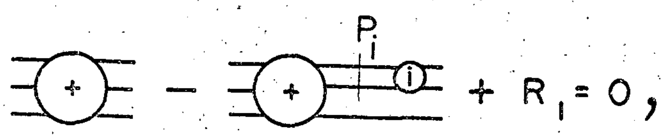

(5.30)

where

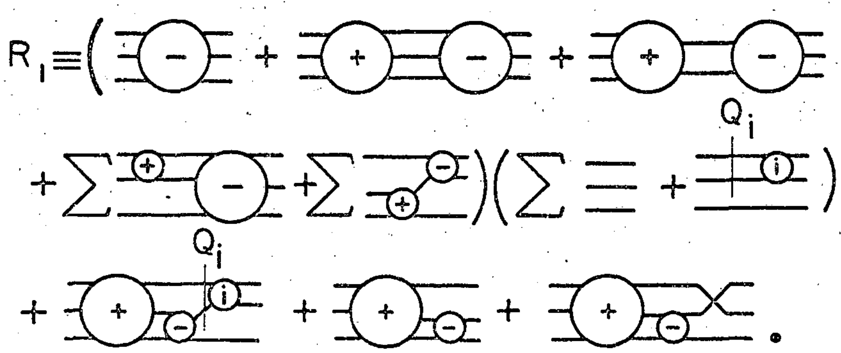

(5.31)

Again setting M_i equal to $\mu_1 + \mu_2$, we see[25] that the only terms of (5.30) that can support D_2 with all α's positive are the first and the second. Thus we obtain[26]

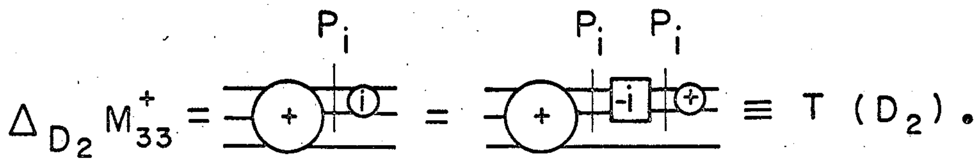

(5.32)

C. Discontinuity Equation for the Ice-Cream-Cone Diagram

To find the discontinuity of M_{33}^{+} across $\mathfrak{M}^{+}[D_3]$ where

$D_3 =$

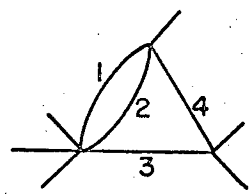

, (5.33)

we first substract (4.1) from (5.30), and obtain

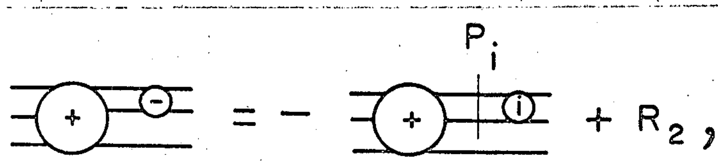

(5.34)

where

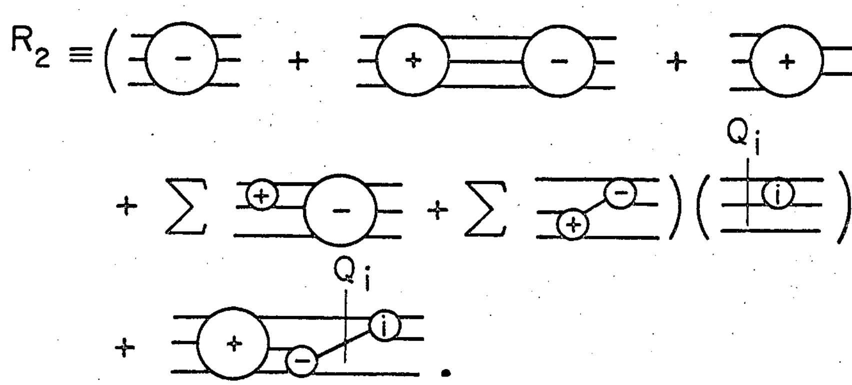

(5.35)

The diagram R_2 cannot support D_2 with all α's positive.[25] Substituting (5.34) into the second term of (4.6) we see[25] that the only terms of (4.6) that can support D_3 with all α's positive are M^+_{33} and $-T(D_3)$ where

$T(D_3) \equiv$ 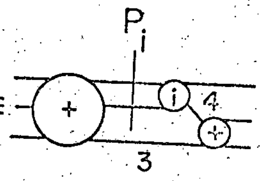

(5.36)

is a threshold term. Thus we obtain[27]

$$\Delta_{D_3} M^+_{33} = T(D_3). \tag{5.37}$$

D. Discontinuity Equation for the Extended Ice-Cream-Cone Diagram

Consider the Landau diagram

$D_4 =$ 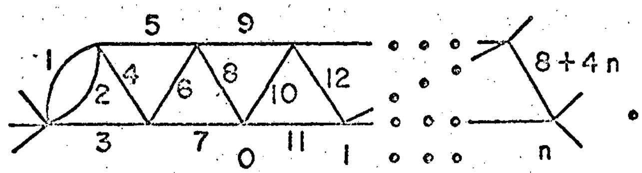

. (5.38)

Substituting (5.34) into the second term of (4.11) we see[25] that the only terms of (4.11) that can support D_4 with all α's positive are M^+_{33} and $-T(D_4)$, where

$T(D_4) \equiv$ 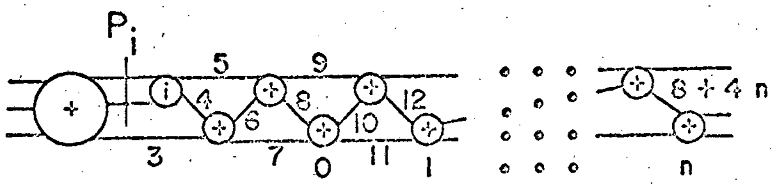

(5.39)

is a threshold term. It therefore follows that

$$\Delta_{D_4} M_{33}^{+} = T(D_4) . \tag{5.40}$$

Similarly, by combining (4.8) and (4.6), or (4.8) and (4.11), and then substituting (5.34), we find that the discontinuity of M_{33}^{+} corresponding to the diagram

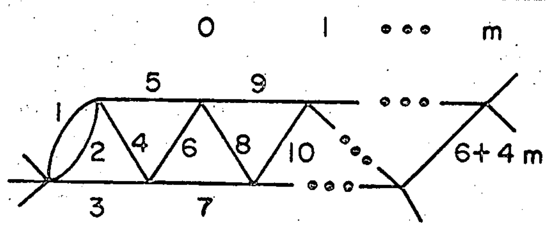

(5.41)

is given by

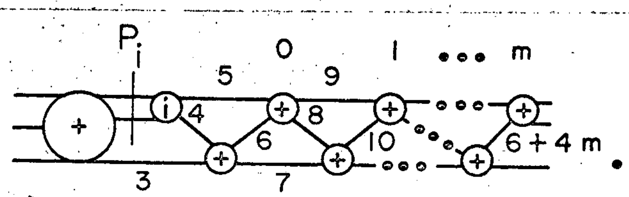

(5.42)

Any set of simple inner vertices (defined in the caption of Fig. 1) of any of the diagrams (5.38) or (5.41) can be replaced by a corresponding set of two-particle closed loops. Then the corresponding discontinuity of M_{33}^{+} is given by (5.39) or (5.42) with every plus bubble corresponding to a two-particle closed loop replaced by the expression (5.26).

E. Discontinuity Equation for Normal Singularities in the Total Energy

The problem is to find the discontinuity of M_{33}^{+} around $\mathcal{M}^{+}[D_5]$ and $\mathcal{M}^{+}[D_6]$ where

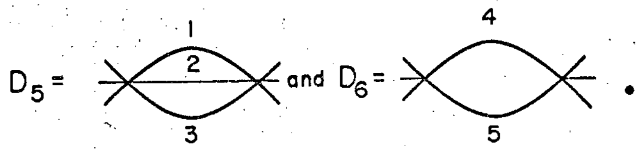

(5.43)

The -i (or F) box was defined in (5.18). By virtue of (2.9) this definition is equivalent to

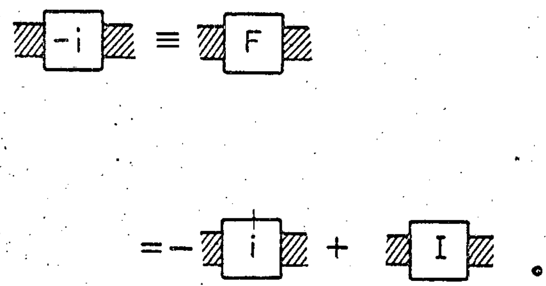

(5.44)

The connected part of the left side of (5.44) is denoted by

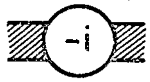

$$\equiv M^{-i}(K';K'') .\qquad (5.45)$$

It then follows from (5.18) and (2.11) that

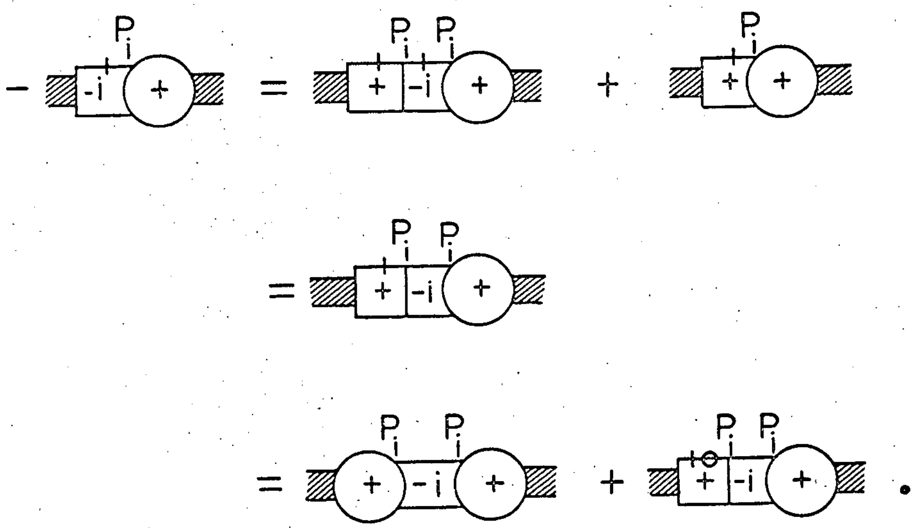

(5.46)

Using (5.20) we can write the connected part of (5.18) in the form

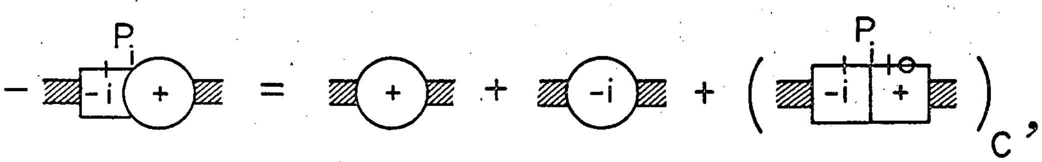

(5.47)

which gives

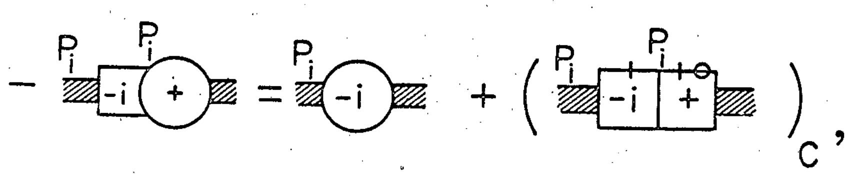

(5.48)

where the subscript C indicates the connected part. Substituting (5.47) and (5.48) into (5.46) we obtain

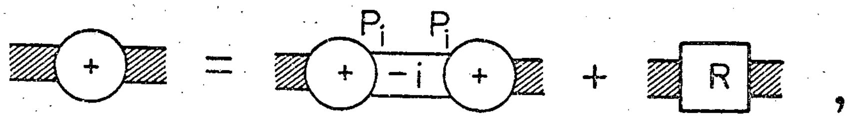

(5.49)

where

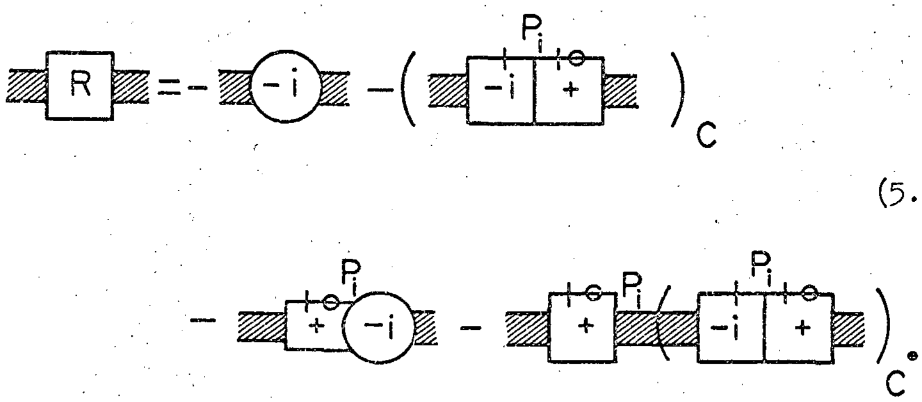

(5.50)

For the special case of three ingoing and three outgoing particles, the terms on the right side of (5.49) are given by

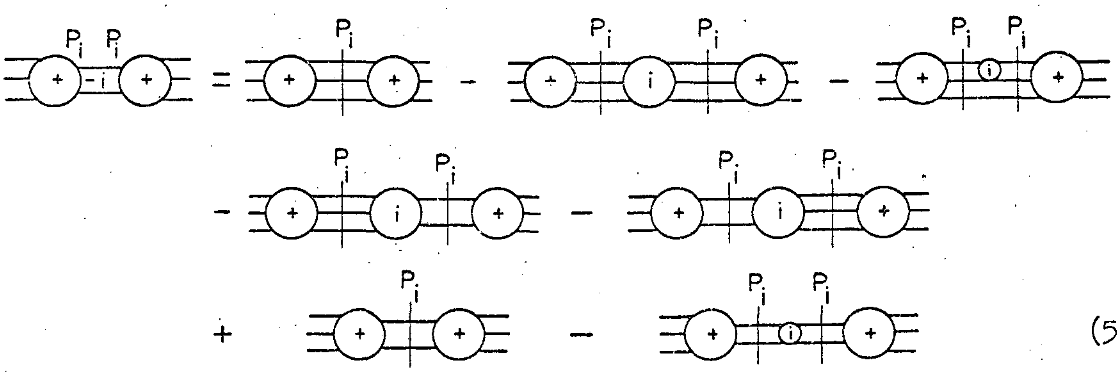

(5.51)

and

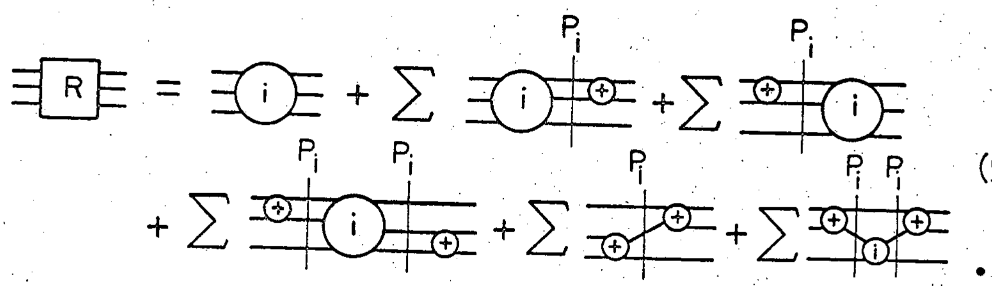

(5.52)

Equation (5.22) is used to obtain the fifth term of (5.52).

The only terms in (5.49) that can support D_5 or D_6 with all α's positive are M^+_{33} and the first term on the right side.[25] Thus, we obtain

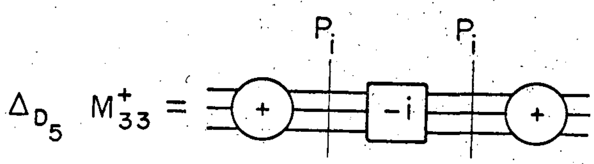

(5.53)

and

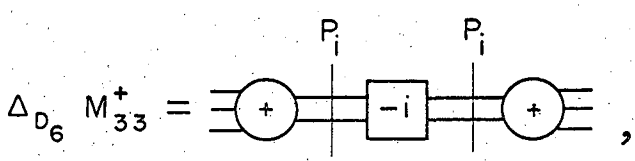

(5.54)

where we set M_i equal to $\mu_1 + \mu_2 + \mu_3$ in (5.53) and equal to $\mu_4 + \mu_5$ in (5.54) and we assume that $\mu_1 + \mu_2 + \mu_3 \neq \mu_4 + \mu_5$. For $\mu_1 + \mu_2 + \mu_3 = \mu_4 + \mu_5$ the discontinuity across $\mathfrak{M}^+[D_5] = \mathfrak{M}^+[D_6]$ is given by

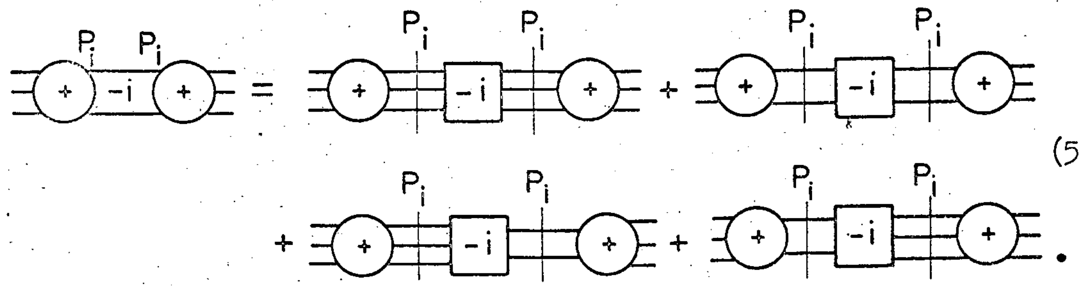

(5.55)

F. Discontinuity Equation for the $3 \to 2$ and $2 \to 3$ Amplitudes

The $3 \to 2$ and $2 \to 3$ amplitudes have no physical-region singularities depending on a cross-energy invariant. The discontinuities of these amplitudes across their singularities are given by formulas completely analogous to those obtained for the $3 \to 3$ amplitude except for the change in the external lines.

G. Equivalent Diagrams

The Landau surfaces corresponding to equivalent (but not identical) diagrams coincide. The discontinuity formulas given by the rules (1.2) of the introduction have partially taken this into account, since a summation over all particles of the same mass M_r is implied for a line labeled with the number r. However, the sum of the rest masses, $M_1 + M_2$, of the particles in a two-particle closed loop may be equal to the sum of the rest masses, $M_1' + M_2' + M_3'$, of the particles in a three-particle closed loop; or it may be equal to the sum of the rest masses, $M_1'' + M_2''$, with $M_1'' \neq M_1$, of another set of particles corresponding the the two-particle loop. The rules

(1.2) do not cover such cases. In the derivations given in this section the possibility of equivalent diagrams is not excluded, and the results cover these cases also. They give, instead of (1.2), the more general rule

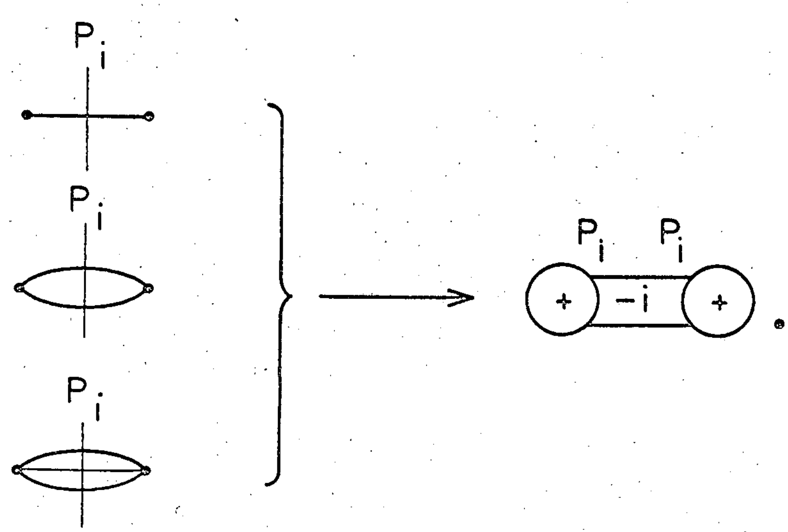

(5.56)

These rules are equivalent to those of (1.2), if there are no equivalent diagrams of the type just mentioned and provided the M_i corresponding to the bar in (5.56) is set equal to the appropriate sum of the masses occurring in (1.2).

It is understood here, as it is in the discontinuity formulas derived in this section, that the bubble-diagram functions on the right side are evaluated just above their threshold. We shall see in the next section that if this restriction is relaxed, then the rule (5.56) can, in some cases, give the discontinuity across a whole set of cuts.

VI. DISCONTINUITY OF THE SCATTERING AMPLITUDE AROUND SEVERAL CUTS

The method used in Section V to derive the discontinuity of M_{33}^{+} across a single Landau surface can be generalized to give the discontinuity across several Landau surfaces.[28]

Consider the set of Landau diagrams

$D_7 =$ 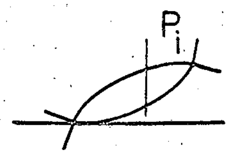

, (6.1)

where the unlabeled internal lines correspond to all possible types of particles that are compatible with the conservation and mass constraints and which satisfy the requirement that the sum of the masses of the particles corresponding to the lines cut by the P_i bar be greater than a given mass M_i. The only terms of (5.30) that can support a Landau diagram of the set D_7 with all α_i positive are the first and the second.[25] On the unphysical side of all the Landau surfaces $\mathfrak{M}^{+}[D_7]$, Eq. (5.30) is $M_{33}^{+} + R_1 = 0$. If this equation is continued to a point that lies on the physical side of all the Landau surfaces $\mathfrak{M}^{+}[D_7]$ in such a way that R_1 is continued into itself, then M_{33}^{+} is continued around $\mathfrak{M}^{+}[D_7]$ according to a minus-iε rule and into a function denoted by $M_{33}^{+}(D_7^{-})$. Subtracting the continued equation from (5.30), we find that the discontinuity $M_{33}^{+} - M_{33}^{+}(D_7^{-})$ is again given by the right side of (5.32).

A similar argument, based on the formulas of subsection V.E shows that the discontinuity of M^+_{33} across the set of Landau surfaces corresponding to the diagrams

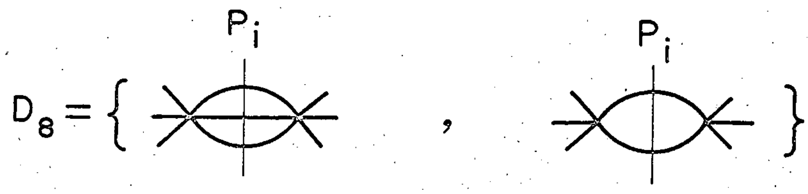

(6.2)

is given by

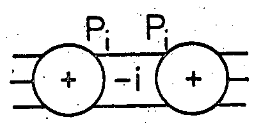

. (6.3)

The same procedure also works for nonnormal singularities. Consider, for instance, the set of Landau diagrams

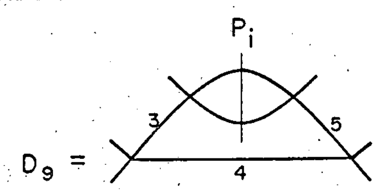

. (6.4)

The discontinuity $M^+_{33} - M^+_{33}(D_9^-)$ across the set of all cuts that begin at the Landau surfaces $\mathfrak{M}^+[D_9]$ is given by the function $T(D_1)$ defined in (5.25), provided we remain in the region where $M^+_{33}(D_9^-)$ has no mixed-α singularities corresponding to D_9 or to the contractions of D_9. This restriction is imposed because the Third Structure Theorem cannot be used to continue the right side of $M^+_{33}(D_9^-) = M^+_{33} - T(D_1)$ into itself around such mixed-α singularities.

Finally, let us examine the total discontinuity of M_{33}^{+} across all normal thresholds in the total energy or in a subenergy. Consider the set of diagrams

$D_{10}=$ 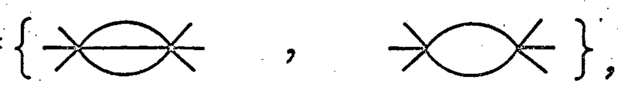 (6.5)

where the unlabeled internal lines correspond to all possible types of particles that are compatible with the conservation and mass constraints. This set is composed of the subsets

$D'_{10}=$ 

(6.6)

and

$D''_{10}=$ 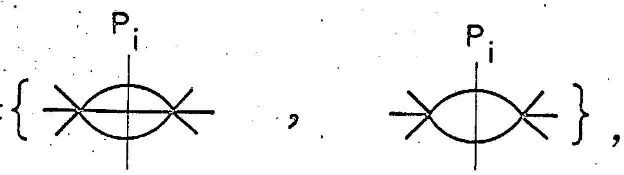

(6.7)

where we choose M_i in such a way that $E = M_i$ is the energy corresponding to the lowest normal threshold lying within the physical region of M_{33}^{+}. (Thus, the normal thresholds corresponding to the diagrams D'_{10} lie outside or on the boundary of the physical region of M^+_{33}.) We define

$M^+_{33}(D'^-_{10}) =$ 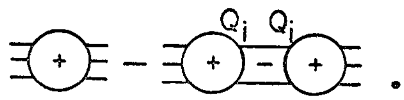

(6.8)

The argument which led from (5.46) to (5.49) also works if we replace $-i$ by a minus sign and omit the P_i bar in these formulas. Then, Eq. (5.49) becomes

(6.9)

where

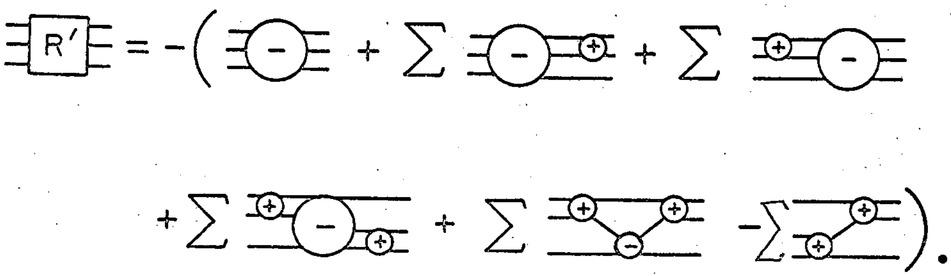

(6.10)

On the unphysical side of the set of singularities corresponding to D''_{10} we see that

$$M^{+}_{33}(D'^{-}_{10}) =$$  , (6.11)

where we have used (6.9). If this equation is continued to a point which lies on the physical side of the surfaces $\mathfrak{M}^{+}[D_{10}]$ in such a way that the right side of the equation is continued into itself, then $M^{+}_{33}(D'^{-}_{10})$ is continued below the cuts corresponding to $\mathfrak{M}^{+}[D''_{10}]$ and into a function denoted by $M^{+}_{33}(D^{-}_{10})$.[25] Subtracting the continued equation from (6.9) we obtain

$$M^{+}_{33} - M^{+}_{33}(D^{-}_{10}) =$$ 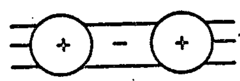 . (6.12)

Equation (6.12) gives discontinuity of M^{+}_{33} across all the Landau surfaces $\mathfrak{M}^{+}[D_{10}]$ provided $M^{+}_{33}(D'^{-}_{10})$ can be regarded as a continuation of M^{+}_{33} to some unphysical sheet.

With a similar proviso, we find that the total discontinuity across the singularities corresponding to the diagram

$$D_{11} =$$ 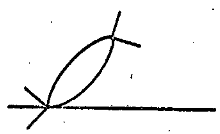 (6.13)

is given by

$$M^{+}_{33} - M^{+}_{33}(D^{-}_{11}) = -$$ 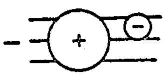 $$=$$ 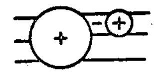 . (6.14)

Equations (6.12) and (6.14) can be regarded as just definitions of $M^{+}_{33}(D^{-}_{10})$ and $M^{+}_{33}(D^{-}_{11})$, respectively. The nontrivial aspect is the result that these functions have minus-$i\epsilon$ continuations around the normal threshold $\mathfrak{M}^{+}[D''_{10}]$ and $\mathfrak{M}^{+}[D''_{11}] \equiv \mathfrak{M}^{+}[D_{7}]$, respectively.

Appendix A. Combinatorics

1. Cluster Decomposition of the S Matrix

For bosons the cluster decomposition property of the S matrix is expressed by

$$M(K'; K'') = \sum_p M_p(K'; K'') \tag{A.1a}$$

and

$$M_p(K';K'') = \prod_{s=1}^{N_p} M_1(K'_{ps} ; K''_{ps}) . \tag{A.1b}$$

The sum over p is a sum over all partitions of the set of variables $(K'; K'')$ into disjoint subsets. The set of variables $(K'_{ps} ; K''_{ps})$ is the sth subset of the pth partition. The pth partition has altogether N_p subsets, and the first partition, $p = 1$, is the unique partition with $N_p = 1$ and $K'_{11} = K'$, $K''_{11} = K''$.

The cluster decomposition is graphically represented in terms of bubble diagrams. A bubble with a plus sign inside represents the connected part, $M_1(K'_{ps} ; K''_{ps})$, of the S matrix $M(K'_{ps} ; K''_{ps})$. Then $M(K'; K'')$ is represented by a sum of terms each of which is a column of plus bubbles. (The set of bubbles includes trivial bubbles, which are bubbles connected to just one initial and one final line). Counting is important. There is precisely one term for each topologically different way of connecting a column of plus bubbles to the given set of external lines specified by $(K'; K'')$. The topological structure is determined completely by specifying the grouping of the external lines into subsets. The lines of each individual subset $(K'_{ps} ; K''_{ps})$ of external lines are drawn as emerging from a single bubble. Two diagrams that differ only in the ordering of the bubbles in the column are not topologically different. Similarly, two diagrams that differ only in the ordering of the lines emerging from any given bubble are not topologically different. This latter fact allows us to always draw the diagrams so that the lines emerging from any given bubble never cross. However, lines emerging from different bubbles may cross. A typical term will thus have a structure like that shown in Fig. 5.

2. Counting the Intermediate States

The unitarity equation is

$$\sum_{K} M(K'; K) \; M^{\dagger}(K;K'') = \delta(K'; K''). \qquad (A.2)$$

Here $K = (p_1, t_1, p_2, t_2, \cdots, p_n, t_n)$ is a set of variables $V_j \equiv (p_j, t_j)$. The sum over K includes a sum over all n. For each n, each of the n indices t_j is summed over all possible values. And for each value of t_j there is an integration over all values of p_j satisfying $p_j^{\,2} = \mu_j^{\,2} \equiv \mu^2(t_j)$. The states are labeled by <u>unordered</u> sets K. That is states labeled by sets K that differ only in the order of the variables of K are not counted as different. Thus, one must either restrict the range of integration by some normal ordering convention, as in Ref. 15, or divide by $n!$. Let us temporarily adopt the latter method, so that there is no restriction on the range of integration. Then the summation on the left side of (A.2) can be written in the explicit form

$$\sum_{K} = \sum_{j=1}^{n} \frac{1}{n!} \sum_{t_1=1}^{\tau} \sum_{t_2=1}^{\tau} \cdots \sum_{t_n=1}^{\tau}$$

$$\times \int \frac{d^4 p_1}{(2\pi)^4} \, 2\pi \; \theta(p_1^{\,0}) \, \delta(p_1^{\,2} - \mu_1^{\,2}) \, \frac{d^4 p_2}{(2\pi)^4} \, 2\pi \; \theta(p_2^{\,0}) \, \delta(p_2^{\,2} - \mu_2^{\,2}) \cdots$$

$$\times \frac{d^4 p_n}{(2\pi)^4} \, 2\pi \; \theta(p_n^{\,0}) \, \delta(p_n^{\,2} - \mu_n^{\,2}) \; . \qquad \text{(A.3)}$$

Here n is the number of lines in the intermediate state, and τ is the number of types of particles. The momentum p_j is associated with line j and also with the type variable t_j and can therefore be written as $p_j(t_j)$.

When we transcribe unitarity (A.2) into bubble notation, we find that topologically indistinguishable diagrams occur. That is, even though the individual M functions are expressed as a sum of topologically different diagrams, the topological product of these diagrams contains diagrams that are not topologically different. The topological structure of a contribution to the product is specified by specifying first which subsets of the set of outgoing variables K' are grouped together (i.e., are attached to a common bubble) and which subsets of the set of incoming variables K'' are grouped together. [The various variables of K' and K'' are always considered as distinct and identifiable. One can, for instance, take all the p_j in K' and K" to have different fixed values.] The various groups of incoming and outgoing variables can be labeled by indices i and f, respectively. These indices i and f label, then, the bubbles of the right and left columns of the product. It is important to note that this labeling does not refer to the position of the bubbles in the column but rather to the sets of external lines connected to these bubbles.

The number of lines connecting bubble i to bubble f is called N_{fi}. The topological structure is specified by these numbers N_{fi}, together with the specifications of the subsets of incoming and outgoing lines labeled by i and f.

Bubble diagrams of the same topological structure give exactly the same bubble-diagram functions. Thus, the product on the left of (A.2) can be expressed in the form

$$F(K'; K'') = \sum_B c_B \overline{M}^B(K'; K''), \tag{A.4}$$

where the sum is over all the topologically different bubble diagrams B contained in the topological product of the two boxes. The coefficient c_B for a diagram with n internal lines is $N_B/n!$, where N_B is the number of diagrams topologically equivalent to B in the topological product of the two boxes, and the factor $1/n!$ comes from (A.3). The bar on $\overline{M}^B$ indicates that, contrary to the convention adopted in the main text (see below), the regions of integration are not restricted by any ordering convention, but are as given in (A.3). We shall show immediately that

$$N_B = n!/\Pi(N_{fi})!. \tag{A.5}$$

This result gives

$$c_B = 1/\Pi(N_{fi})!, \tag{A.6}$$

the product being over all pairs (f,i). As usual one takes $0! = 1$.

To derive (A.5) one first labels the intermediate lines in accordance with their topological character: Each line is labeled by a unique triple (f,i,m), where f and i label the final and initial bubbles that the line joins, and for any particular values of f and i the m in (f,i,m) is an index that runs from 1 to N_{fi} and specifies the particular one of these N_{fi} lines. There is also the index j that runs from 1 to n, and identifies the n variables of $K = (p_1, t_1, p_2, t_2, \ldots, p_n, t_n)$.

For definiteness, one may specify that the ordering of the lines of any box reading from top to bottom is the same as the ordering of the associated variables of the corresponding set K. Thus, j specifies the geometric location of the intermediate line L_j, reading from top to bottom of the box. The index m of (f,i,m) may also be considered to specify the position, reading from top to bottom, of line (f,i,m) relative to the other lines of the set of lines Γ_{fi} that joins bubbles i and f. The condition imposed earlier that lines attached to a given bubble do not cross within the box insures that the ordering of the lines of Γ_{fi} is well-defined; the relative ordering within one box of any set of lines of Γ_{fi} is the same as the ordering of this set of lines in the other box. This condition that the ordering of the lines Γ_{fi} be given by m is, however, the only restriction on the ordering of the intermediate lines; one readily confirms that the various intermediate lines, as identified by their topological indices (f,i,m), can occur in any possible order (reading from top to bottom), subject only to this condition that the relative ordering of lines in the various sets Γ_{fi} be in accordance with the index m. The term coming from each of these allowed orderings is a different contribution to the product (A.2). Thus, in this product, the number of different contributions that are topologically equivalent to a diagram B is just the number of different allowed orderings of these intermediate lines. This is just the total number of orderings $n!$ divided by the product of the number of orderings within each set Γ_{fi}. Thus we obtain (A.5).

In the text it was specified that the region of integration in the definition of bubble-diagram functions M^B be restricted so that contributions from topologically equivalent diagrams are counted only once. In the derivation of (A.4) no such restriction on the range of integration was imposed, and the corresponding functions were written as $\bar{M}^B$. These two functions are related by the factor c_B. The point here is that the various lines of a set of lines connecting a given pair of bubbles are regarded as topologically equivalent. Thus, in computing M^B, the integration region is restricted so as to include only one of the set of contributions obtained by interchanging the lines of such a set. This restriction on the domain of integration in the definition of the functions M^B means that the $\bar{M}^B$ in (A.4) divided by $\Pi N_{fi}!$ is just M^B. Thus, in place of (A.4) one obtains

$$F(K'; K'') = \sum_B M^B(K'; K''). \tag{A.7}$$

The notion of topological distinctness has been applied on two different levels: When in (A.4) or (A.7) we say the sum over diagrams B is over topologically different diagrams B, we are considering B to be simply a collection of lines and bubbles joined to give a geometric figure; the lines are not yet assigned particular variables. But when for a fixed B we say that the integration region defining M^B is restricted so that topologically equivalent diagrams are counted only once, then we are considering variables (p_j, t_j) to be assigned to the lines. This separation into two levels is evidently arbitrary.

The proof given above can be shortened and extended to products of arbitrary numbers of boxes by arguing as follows. In the integration corresponding to the sum over the set of intermediate states, one is supposed to count only one of the set of possible contributions obtained from the various possible reorderings of the variables. A reordering of variables corresponds to a reordering of the lines associated with the intermediate particles. Thus, the ordering of the intermediate lines can be considered to be completely irrelevant; the intermediate lines can be identified by the value of the associated variables alone. For every way of connecting the various bubbles of the various adjacent columns by lines, and assigning a fixed variable to each line, there is at least one contribution to the overall function. We now define diagrams with fixed variables attached to each line to be topologically equivalent if and only if they can be made identical by some reordering of the various bubbles within the various columns. It then follows that the contributions from two topologically equivalent diagrams should not both be counted. For they must both arise from contributions to the individual boxes that are topologically equivalent, and hence identical. On the other hand, no two contributions that are not topologically equivalent in this sense can come from a single set of contributions from the various boxes. Hence the restriction to topologically different diagrams leaves one with precisely one complete set of independent contributions.

The consequence of this argument is that the function corresponding to a product of any number of functions S and $S^{\dagger}$, with the intermediate sums defined as in the unitarity equations, is represented by the function M^{B}, where B is the natural topological product of the boxes representing the individual functions S and $S^{\dagger}$. One can decompose the various boxes into sums of terms represented by different columns of bubbles. The natural topological product does not include diagrams that are topologically equivalent in the sense that they differ only in the ordering of bubbles within a column or by the path followed by intermediate lines. [Only the end points of the lines are significant.] For each diagram B of the natural topological product there is one term M^B. In evaluating this term the integration is restricted so that topologically equivalent contributions are counted precisely once, where now each line is identified by a variable $(t_j\ p_j)$.

3. Example

In the main text the combinatoric questions are automatically taken care of by the use of functions M^B; the restriction on the ranges of integrations of these functions makes everything correct. To exhibit the combinatoric questions resolved by this notation, and to confirm our basic formulas, we rederive the formulas of Sec. IV starting directly from Eqs. (A.1), (A.2), and (A.3), and using, instead of the functions M^B rather the functions $\overline{M}^B$, which have no restriction on the domain of integration.

First consider two-particle unitarity. The two-particle box is given by

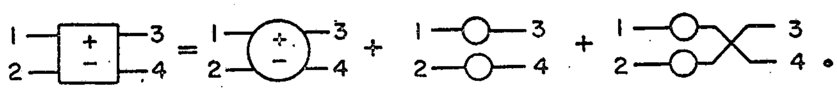

(A.8)

In (A.8) the incoming and outgoing lines are identified redundantly both by an integer and also by the vertical position of the external end points. In the remainder of this appendix we will suppress the integer and use only the latter method of labeling. Below the three-particle threshold we obtain

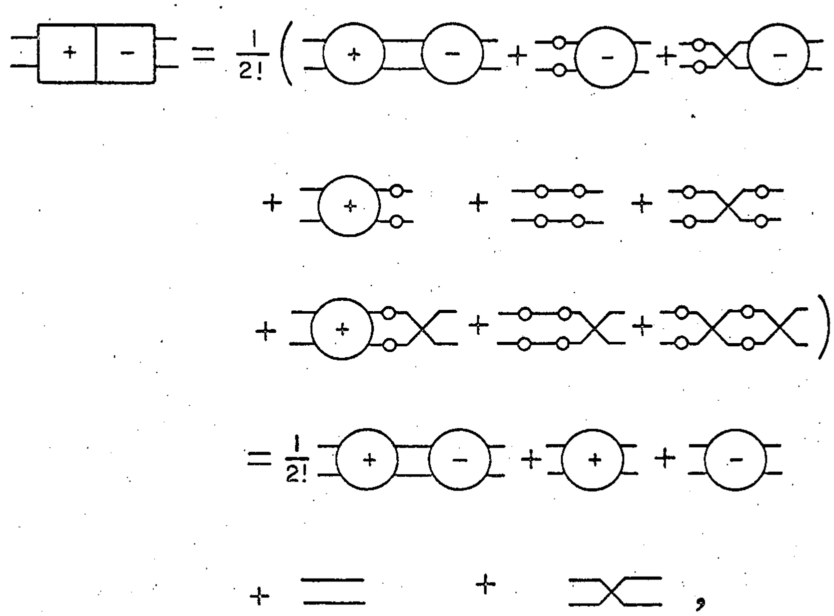

(A.9)

where the factor 1/2! comes from (A.3). [This factor 1/2! does not appear in the equations of the text because there the diagrams represent always the function M^B whereas in this section they represent the functions $\overline{M}^B$.] Equation (A.9) is evidently in agreement with (A.4). The last two terms on the right side of (A.9) are equal to the identity

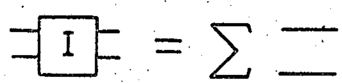

(A.10)

so that the connected part of the unitarity equation is

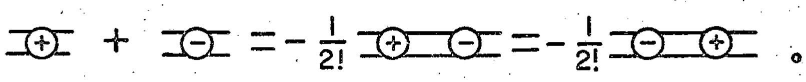

(A.11)

By a completely analogous procedure we obtain, after combining various terms,

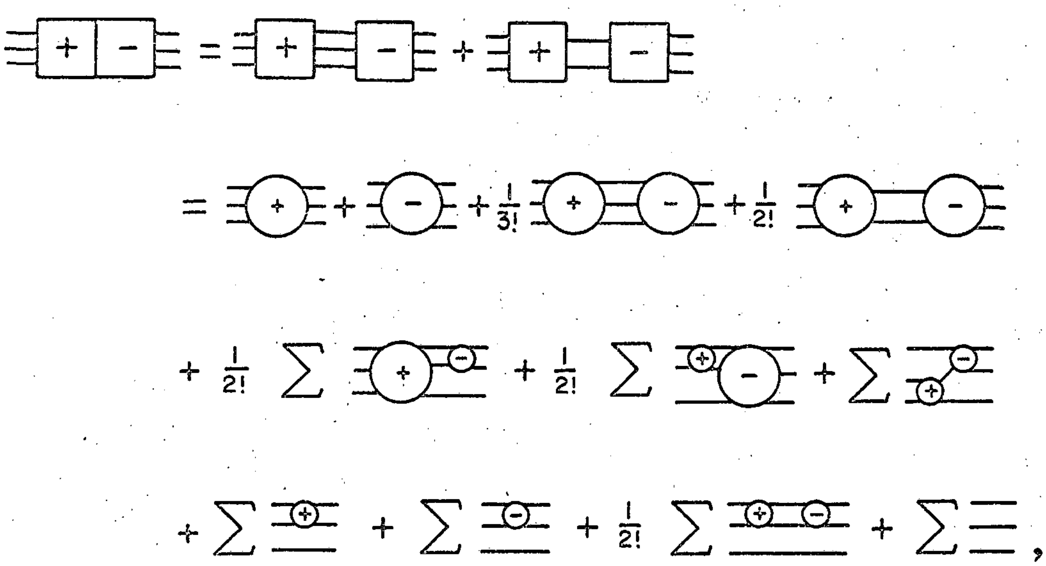

(A.12)

where the summation signs are interpreted as in Section IV. The disconnected parts of (A.12) are equal to the identity by virtue of (A.11), so that the connected part of (A.12) vanishes.

To obtain (4.6) when there is no restriction on the range of integration, we postmultiply the connected part of (A.12) by

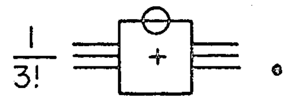

(A.13)

Consider, for instance, the postmultiplication of the nine dumbbell terms of (A.12),

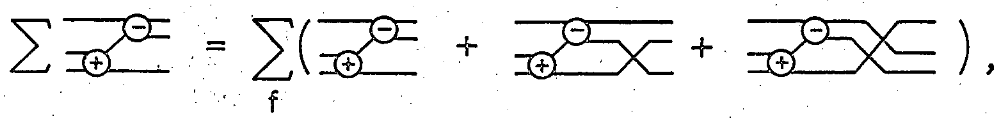

(A.14)

by the $6 + 9$ terms of

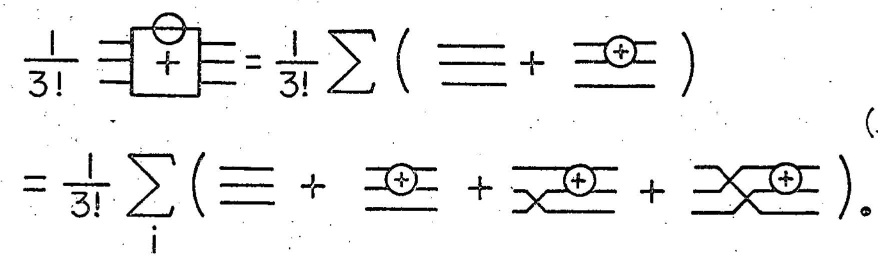

(A.15)

The result of the multiplication is

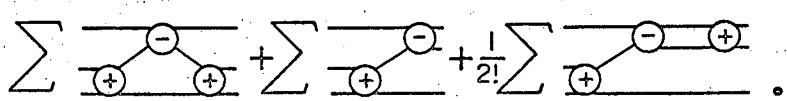

(A.16)

The last two terms combine to give

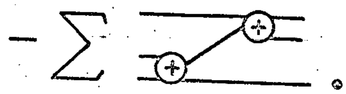

(A.17)

Similarly, the postmultiplication of the terms

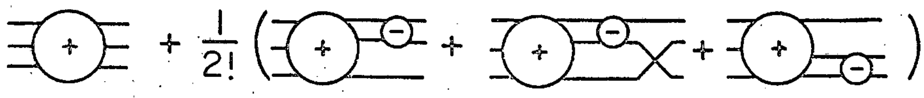

(A.18)

of (A.12) by (A.13) gives

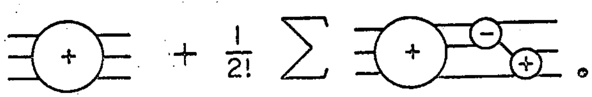

(A.19)

These results check with (4.6) if we take account of the factors $N_{fi}!$ that relate $\bar{M}^B$ to M^B.

Using (A.11) we obtain

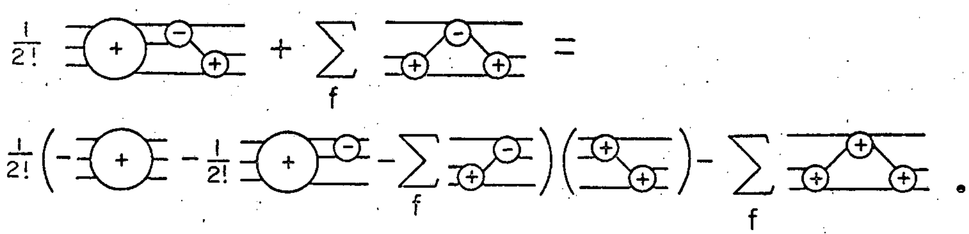

(A.20)

Substituting the unitarity equation

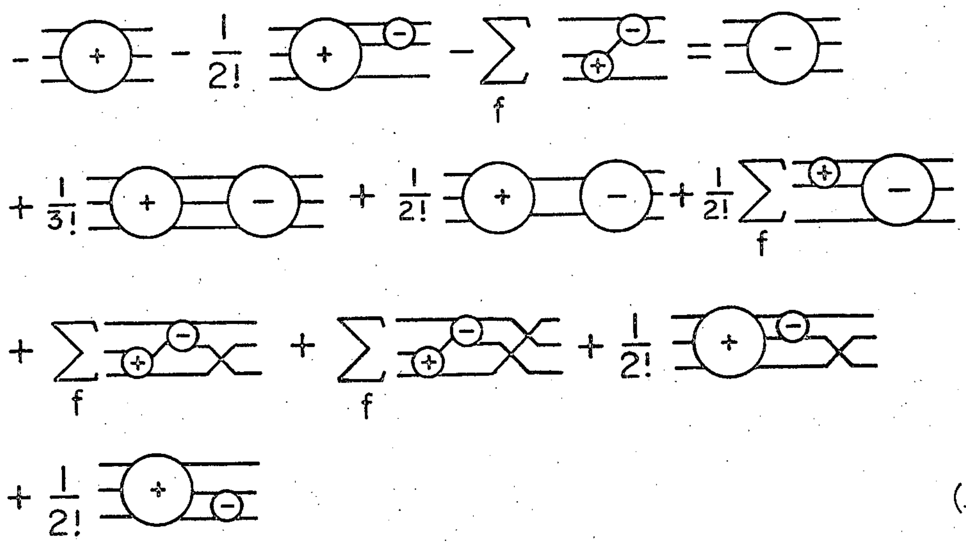

(A.21)

into (A.20) we obtain

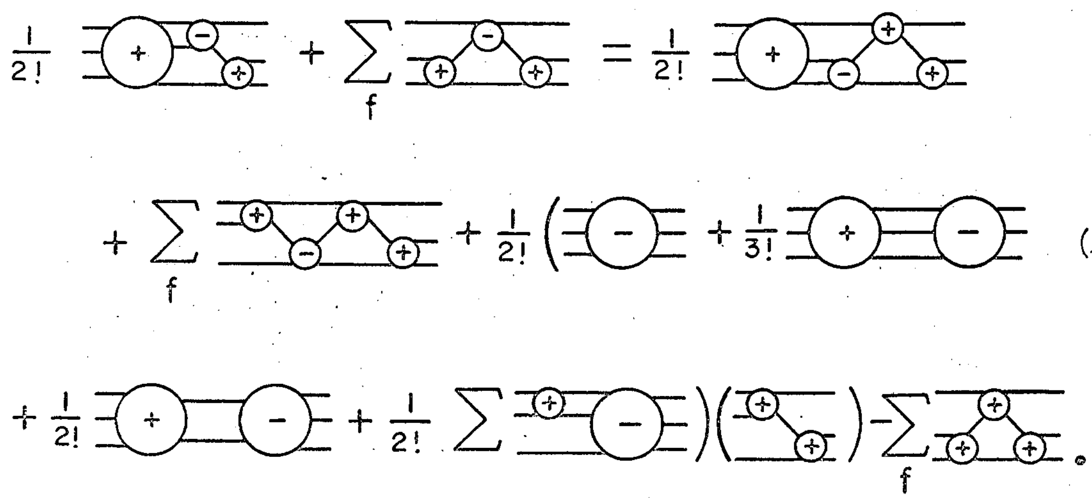

(A.22)

Equations (A.20) and (A.22) check with Eqs. (4.7) and (4.8) of the text if the factors $N_{fi}!$ relating $\bar{M}^B$ to M^B are considered.

The remaining equations of Section IV now follow from the equations already derived and pose no combinatorial problems.

Appendix B. Determination of $M^i(K';K'')$ Using Fredholm Theory[29]

The $M^i(K';K'')$ are defined by (5.8). Let us first assume that $E < M_i$. Then a comparison of (5.8) and (5.6) shows that

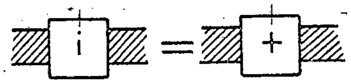

(B.1)

and that (5.19) must hold. Thus, (5.8) can be written in the form

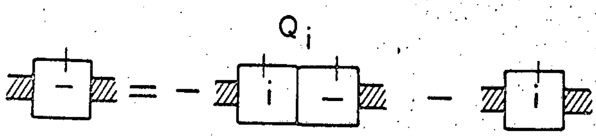

(B.2)

Let us now postmultiply (B.2) by

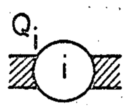

(B.3)

and go through exactly the steps that led from (5.46) to (5.49), but making the replacements

$$+ \to i, \quad -i \to -, \quad P_i \to Q_i \, . \qquad \text{(B.4)}$$

Then in place of (5.49) we obtain

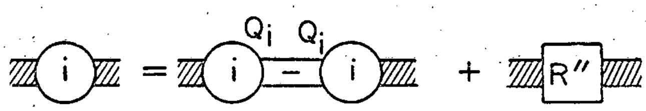

(B.5)

where

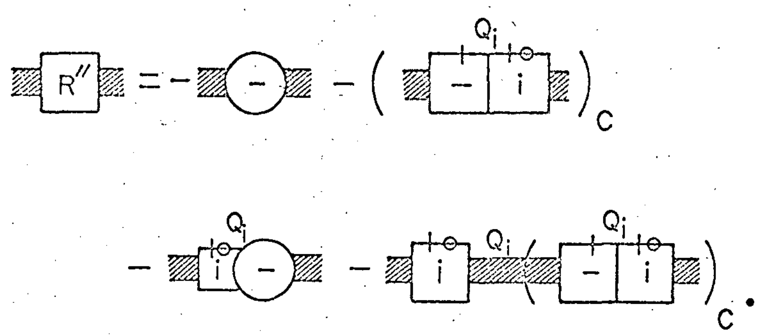

(B.6)

The connected part of (5.8), premultiplied by Q_i, can be written in the form

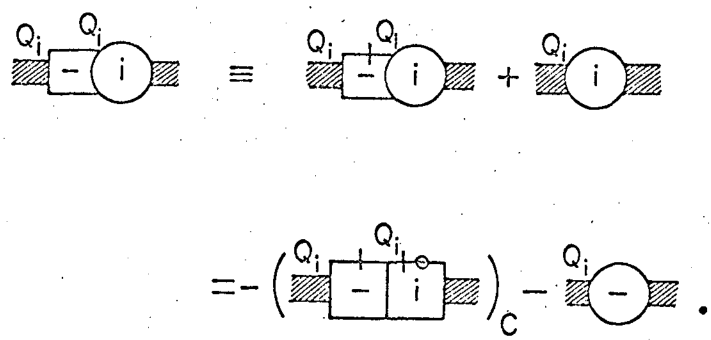

(B.7)

Substituting (B.7) into (B.5) we obtain

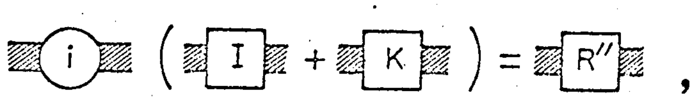

(B.8)

where

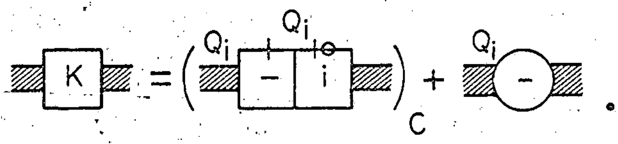

(B.9)

The kernel of the integral equation (B.8) is given in explicit form by the equations

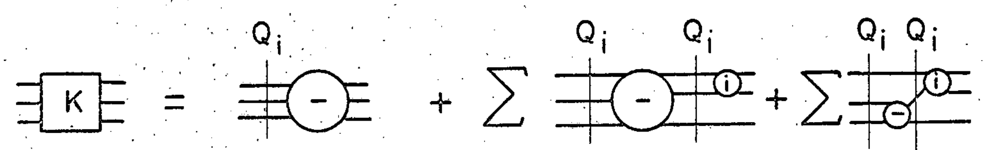

(B.10)

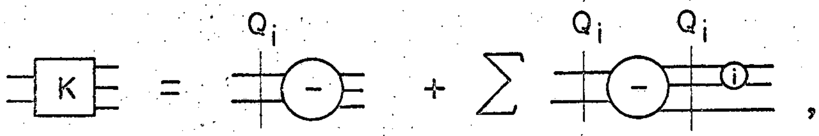

(B.11)

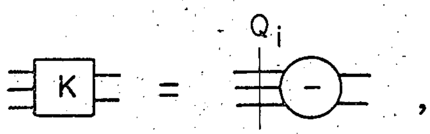

(B.12)

and

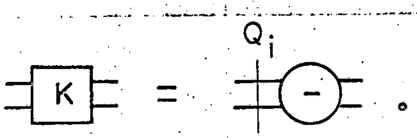

(B.13)

The delta function appearing in (B.10) combines with the remaining terms of this equation to give a pole with a plus-$i\epsilon$ rule. This follows from an argument similar to that used by Olive, except that one uses (5.21) rather than (4.5) to combine the residues of the poles.[30] The contour of integration can be distorted away from the remaining singularities of the kernel.[31] Thus Eq. (B.8) can be solved for $M^i(K';K'')$ through the Fredholm formula.

Using Eq. (5.21) we can express the right side of (B.8) in the explicit form

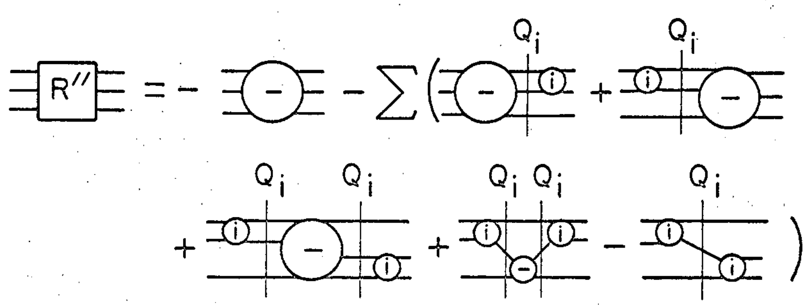

(B.14)

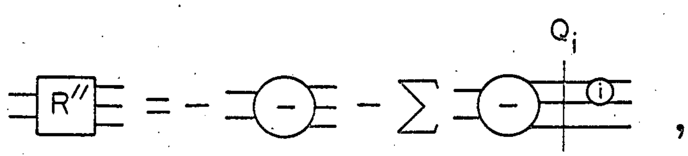

(B.15)

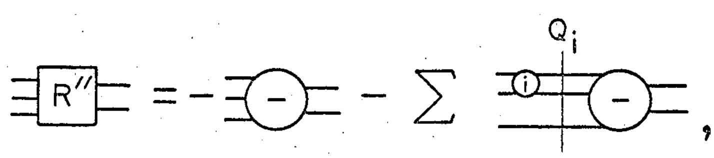

(B.16)

and

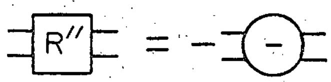

(B.17)

We suppose that (5.21) has been solved already for M^i_{22} and that this solution has been substituted in (B.14), (B.15), and (B.16), as well as in (B.10) and (B.11). It is then seen that the Fredholm solution of (B.8) expresses M^i_{33}, M^i_{23}, and M^i_{32} in terms of bubble-diagram functions all of which follow a minus-iε prescription at the normal two- or three-particle threshold at $E = M_i$. It then follows[31] that the solution $M^i(K';K'')$ of (B.8), and moreover Eq. (5.8) itself, can be analytically continued from $E < M_i$ to $E > M_i$ by following a minus-iε rule.

The original restriction to $E < M_i$, which we used to justify (B.2), entails that the set of incoming particles and the set of outgoing particles each have a sum of rest masses less than M_i. Thus these sets are, in effect, cut by a Q_i bar. Hence the Fredholm solution of (B.8) is an explicit expression for

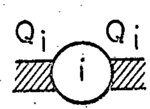

(B.18)

for $E < M_i$ that has a minus-iε rule for continuation past the normal threshold at $E = M_i$. In Appendix C we will enlarge upon this result and show that Eq. (B.8) determines also $M^i(K';K'')$. (That is, the Q_i bars can be omitted.)

The fundamental result established above is that the physical scattering function has a continuation past the normal-threshold singularity in the minus $i\epsilon$ sense, apart from possible poles coming from the vanishing of the Fredholm denominator. Discounting the possibility that these poles become dense,[32] we obtain, using the same arguments that led to the Third Structure Theorem, the result that all terms in (5.8) can be continued in the minus-$i\epsilon$ sense around the normal threshold at $E = M_i$. Thus, this equation can be regarded as valid on both sides of $E = M_i$, with $M^i(K';K'')$ a function that has a minus-$i\epsilon$ continuation around the singularity at $E = M_i$.

Appendix C. Proof of Equation (5.19)

In Appendix B we showed that the equation

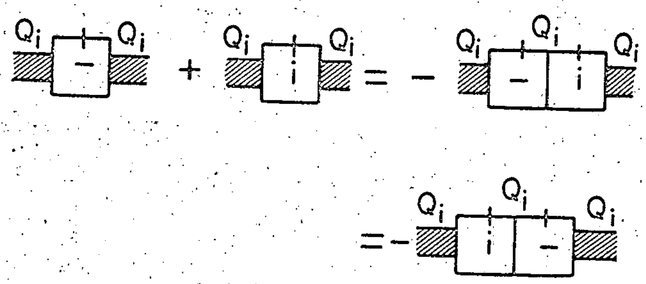

(C.1)

valid for $E < M_i$ can be analytically continued to the region $E > M_i$. We now show that Eq. (5.19) is a consequence of (C.1) and the definition (5.8).

It follows from (C.1) and (5.8) that

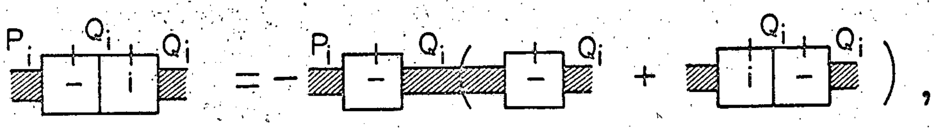

(C.2)

and

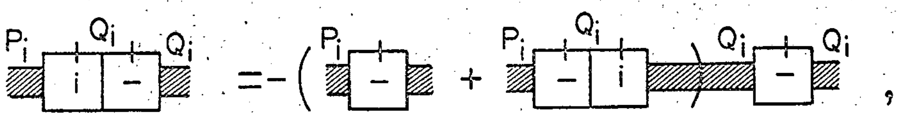

(C.3)

and also that

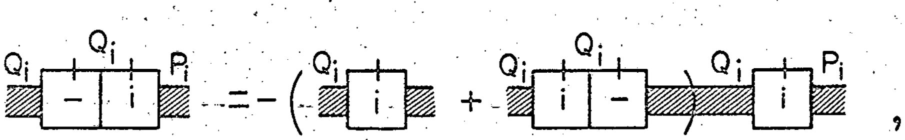

(C.4)

and

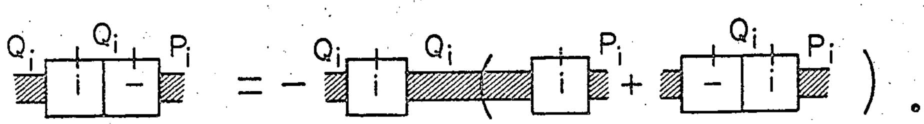

(C.5)

Comparison of the right sides shows that the left side of (C.2) is equal to the left side of (C.3), and that the left side of (C.4) is equal to the left side of (C.5). Using this result and Eq. (5.8) we obtain

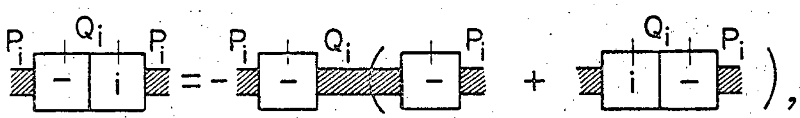

(C.6)

and

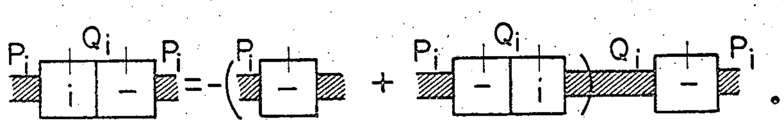

(C.7)

Since the right sides are equal, so are the left sides, and hence the proof of (5.19) is complete.

Since Eq. (B.8) was based on (5.8), (5.19), and nothing else, we see that (B.8) can be used to determine

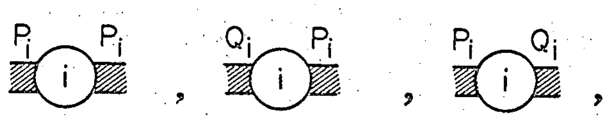

(C.8)

as well as

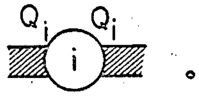 (C.9)

Alternatively, we can determine the quantities (C.8) in terms of (C.9) by directly using (5.8) and (5.19). Thus, we may write

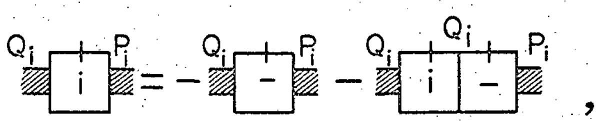 (C.10)

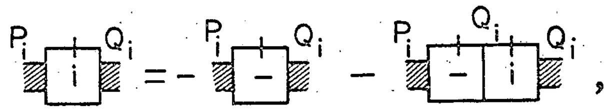 (C.11)

and

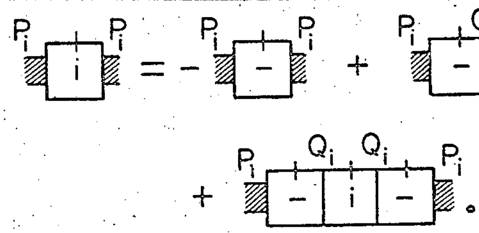 (C.12)

Appendix D. The F_{nm} as Sheet Converters

The right sides of the discontinuity equations given in the previous sections are expressed in terms of plus bubbles and F boxes. These boxes are defined in terms of physical scattering amplitudes by Fredholm integral equations. It is shown in this appendix that the effect of applying a (nontrivial) F box to the physical scattering amplitude is to convert the latter to its value on the unphysical side of a certain cut. This result allows one to express the discontinuity formulas in all cases considered in this paper in terms of the scattering amplitudes evaluated on various sheets, instead of in terms of physical amplitudes and F boxes. The proof depends, however, on the so-called extended unitarity equations.

In the main text we have been careful to use only physical unitarity equations. In particular, the various momentum vectors are always real, apart from infinitesimal variations needed in the continuation around Landau singularities. This restriction means that the unitarity equations below a certain threshold in the total energy at $E = M_i$ hold only if the sums of the rest masses of the initial and final particles are both less than M_i. There are similar restrictions on the masses of subsets of initial and final particles associated with subenergies. The equations obtained if one relaxes these conditions are called extended unitarity equations. Their justification within the S-matrix framework is discussed in Refs. 13, 30, and 33. In this appendix these extended unitarity equations are assumed without further comment.

Consider first the set of Landau diagrams

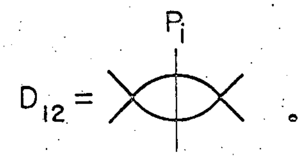

(D.1)

From (5.22) and the fact that M^{i}_{22} has a minus-iε continuation past $\mathcal{M}^{+}[D_{12}]$, we obtain

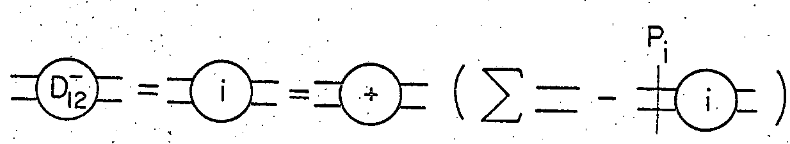

(D.2)

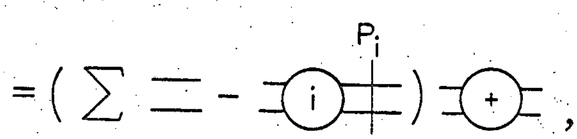

(D.2')

where

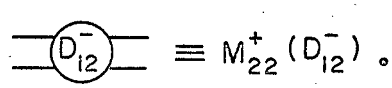

(D.3)

This derivation depends on the assumption that the region $E < M_i$ contains physical points. That is, within the framework of the physical unitarity equations, the derivation of (D.2) and (D.2') is only justified if the set of incoming particles and the set of outgoing particles, each has a sum of rest masses smaller than M_i.

This restriction can be represented by placing Q_i bars on the external lines. By virtue of the extended unitarity assumption, this restriction can be dropped, and one obtains as special cases of (D.2) and (D.2') the results

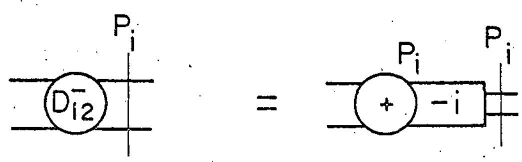

(D.4)

and

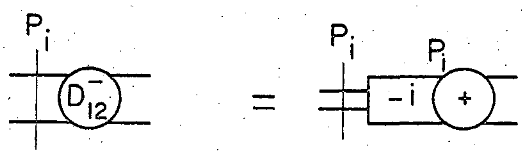

(D.4')

Similarly, using the results of Sec. VI, we find that

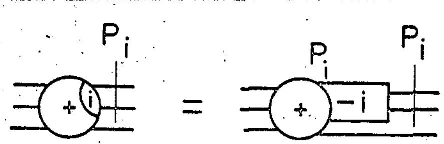

(D.5)

where

$M^+_{33}(D^-_7) \equiv$ 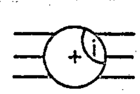

(D.6)

Next consider the set of Landau diagrams

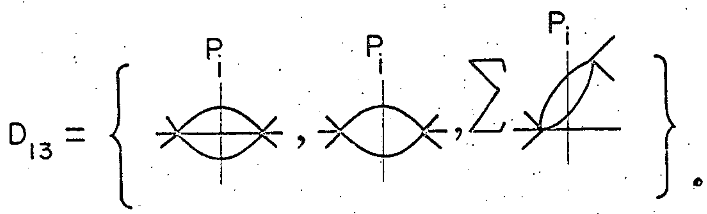

(D.7)

The discontinuity around the set of Landau surfaces $\mathfrak{M}^{+}[D_{13}]$ is derived, according to the method of Sec. VI by noting that the connected part of (5.18) can be written in the form

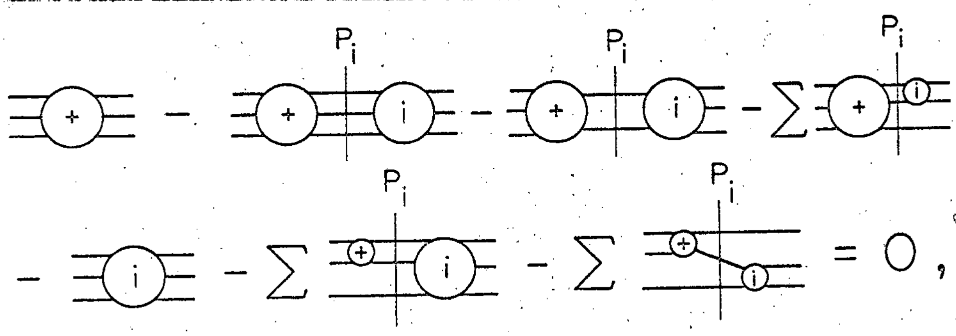

(D.8)

where only the first four terms can support a diagram of the set D_{13} with all α's positive. Thus we obtain

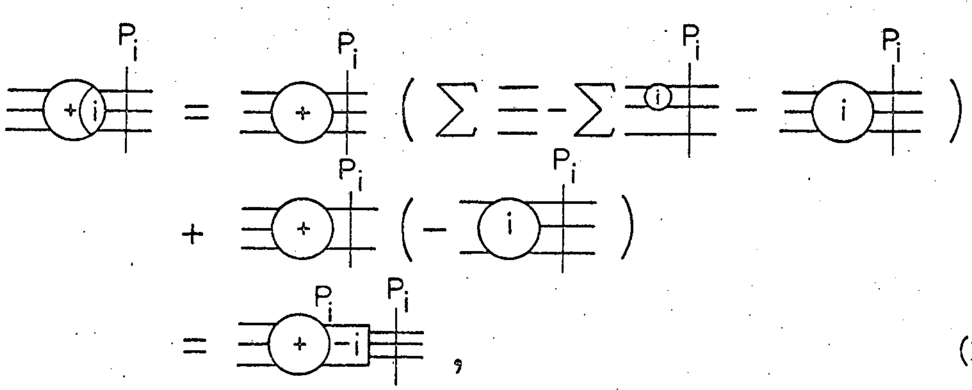

(D.9)

where

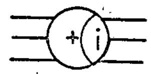

$$\equiv M^{+}_{33}(D^{-}_{13}) . \qquad \text{(D.10)}$$

Using similar methods we can establish the more general results

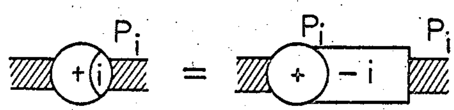

(D.11)

and

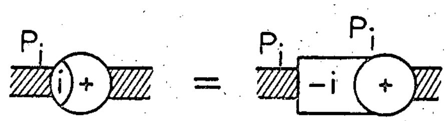

(D.12)

Formulas (D.4), (D.4'), (D.5), (D.11), and (D.12) can be substituted on the right side of the various discontinuity equations derived earlier. The F boxes are thereby eliminated, but the scattering functions are evaluated on unphysical sheets.

Appendix E. Proof of the Absence of Certain Positive-α Landau Singularities in Certain Bubble-Diagram Functions

In this appendix we prove that certain sets of bubble diagrams occurring in the equations of the main text and in Appendix D cannot support certain Landau diagrams with all α's positive. We say that a bubble diagram B cannot support a diagram D with all α's positive if and only if M^B has no singularity surface $\mathfrak{M}^+[D]$. This means, specifically, that if the signs of the α's are restricted in accordance with the Second Structure Theorem, then the Landau equations for $D \supset\subset B$ have no positive-α solution.

Consider first the Landau diagram D_2 defined in (5.27) and the set of bubble diagrams R_1 defined in (5.31). Let each M^i_{22} occurring in R_1 be replaced by the right side of (5.13). Since we are interested only in Landau diagrams with all α's positive, all minus bubbles in R_1 can be replaced by point vertices. Then the function M^i_{22} can also be replaced by a point vertex since none of the internal lines shown in the right side of (5.13) can be a line of D_2. It is seen by inspection that no term in R_1, except possibly contributions of the type

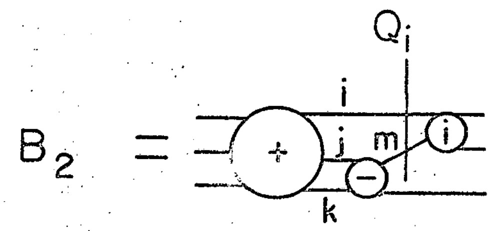

, (E.1)

can support D_2 with all α's positive. (The letters labeling the internal lines in (E.1) stand for a specific set of integers.) Clearly the bubble diagram B_2 cannot support D_2 with all α's positive if line m is contracted. Thus, this line must be one of the two internal lines of D_2. The other line of D_2 cannot be i, because of the projection Q_i. Nor can the remaining line of D_2 be line j (or k) for the resulting Landau loop equation $\alpha_j p_j + \alpha_m p_m = 0$ cannot be satisfied with all α's and all $p_r{}^o$ positive. Finally, the second line of D_2 cannot be an internal line of the $3 \rightarrow 3$ plus bubble because the stability requirement would then force one final external line to emerge from the right-hand vertex of D_2, contrary to its definition. Thus all the possibilities are eliminated, and B_2 cannot support D_2 with all α's positive. Hence neither can R_1.

Next consider the diagram D_3 defined in (5.33). After carrying out the substitutions specified in section V.C., we see by inspection that no term of (4.6), except M^+_{33}, $T(D_3)$, and possibly contributions of the type

$B_3 =$ 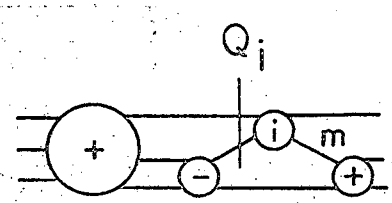

, (E.2)

can support D_3 with all α's positive. Line m of B_3 cannot be contracted and must be line 4 of D_3. Then applying the same arguments as above, we conclude that B_3 cannot support D_3 with all α's positive. Similar arguments can be made for the extended ice-cream cone diagram.

Consider next the diagram D_5 defined in (5.43). The $3 \to 3$ i bubble occurring in (5.52) cannot support D_5 with all α's positive. This follows by considering the right side of (5.12), a typical term of which is

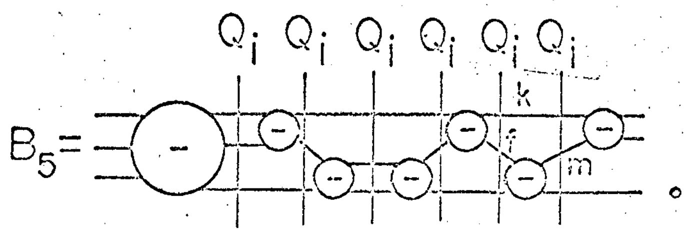

(E.3)

All the bubbles of B_5 can be contracted to points. Line m must evidently also be contracted if one is to obtain D_5. One then sees that any way of picking out three internal lines of B_5 such that the contraction of all others leads to a diagram with the structure of D_5 is such that these three lines are cut by the same Q_i bar of B_5. But then these three lines cannot be lines 1, 2, and 3 of D_5, and hence B_5 cannot support D_5 with all α's positive. Similar arguments show that none of the terms on the right side of (5.52) can support D_5 or D_6 [or in fact any of the diagrams of D_8 defined in (6.2)] with all α's positive.

The $3 \to 3$ i bubble cannot support the last diagram, D'_{13}, on the right side of Eq. (D.7) with all α's positive. To see this consider again the typical term B_5. Evidently D'_{13} cannot be obtained if m is contracted. Thus m must become one of the two internal lines of D'_{13}. The second one cannot be f, because the Landau equations are not then solvable with positive α_j's and p_j^0's. Thus the second line of D'_{13} must be line k of B_5. Then B_5 cannot support D'_{13} with all α's positive because of the restrictions imposed by the Q_i bar. Similar arguments show that the last two terms on the left of (D.8) cannot support D'_{13} with all α's positive.

Because minus bubbles can be contracted to points, we see that no term on the right side of (6.10) can support a diagram of the set D''_{10} with all α's positive.

FOOTNOTES AND REFERENCES

* This work was done under the auspices of the U. S. Atomic Energy Commission.

1. R. E. Cutkosky, J. Math. Phys. 1, 429 (1960); Phys. Rev. Letters 4, 624 (1960).
2. J. Gunson, Birmingham preprint (1962) and J. Math. Phys. 6, 827, 845, 852 (1965).
3. H. P. Stapp, Lectures on Analytic S-Matrix Theory (Matscience, Madras, India, 1963), and Discontinuity Equations, Trieste Report IC/65/17.
4. D. I. Olive, Nuovo Cimento 37, 1422 (1965).
5. R. C. Hwa, Phys. Rev. 134, B1086 (1964).
6. P. V. Landshoff and D. I. Olive, J. Math. Phys. 7, 1464 (1966).
7. P. V. Landshoff, D. I. Olive, and J. C. Polkinghorne, J. Math. Phys. 7, 1593 (1966).
8. P. V. Landshoff, D. I. Olive, and J. C. Polkinghorne, J. Math. Phys. 7, 1600 (1966).
9. M. J. W. Bloxham, Nuovo Cimento 44A, 794 (1966).
10. J. K. Storrow, Nuovo Cimento (in press).
11. C. Chandler and H. P. Stapp, S-Matrix Causality Conditions and Physical-Region Analyticity Properties (in preparation).
12. F. Pham, CERN preprint (1966).
13. H. P. Stapp, Crossing, Hermitian Analyticity, and the Connection Between Spin and Statistics, Lawrence Radiation Laboratory Report UCRL-16816, April 1966 (submitted to Journal of Mathematical Physics).

14. D. Branson, Nuovo Cimento 44A, 1081 (1966).

15. The inclusion of spin is a trivial complication in the M-function formalism. See H. P. Stapp, Phys. Rev. 125, 2139 (1962); The Analytic S-Matrix Framework, in "The Trieste Lectures", High Energy Physics and Elementary Particles (IAEA, Vienna, 1965).

16. See Ref. 13 for a discussion of the necessary phase factors in the Fermi case.

17. A similar result was obtained by J. C. Polkinghorne, Nuovo Cimento 25, 901 (1962).

18. In Ref. 13 trivial Landau diagrams were not included among the set of Landau diagrams.

19. An independent derivation of this representation was given by A. A. Logunov, I. T. Todorov, and N. A. Chernikov in the Proceedings of the 1962 International Conference on High Energy Physics at CERN (CERN, Geneva, 1962), p. 695.

20. A similar result was obtained by P. V. Landshoff and D. I. Olive in the appendix of Ref. 6.

21. A subenergy is the energy of a proper subset of initial or final particles in its own center-of-mass frame. A cross-energy invariant is the square of the sum of the momentum-energy vectors of a set of particles that contains both initial and final particles. The eight invariants needed to describe a $3 \to 3$ reaction are chosen to include two initial subenergies, two final subenergies, and the total center-of-mass energy E of the

reaction. Then all six subenergies are functions only of these five invariants and are therefore independent of the remaining three variables, which are cross-energy invariants. The choice of the invariants is discussed by V. E. Asribekov, Zh. Eksperim. i Teor. Fiz. 42, 565 (1962) [English translation: Soviet Phys.-JETP 15, 394 (1962)].

22. H. P. Stapp, Finiteness of the Number of Positive-α Landau Surfaces in Bounded Portions of the Physical Region, Lawrence Radiation Laboratory Report UCRL-17219, October 1966 (to be published in J. Math. Phys.).

23. Cf. J. Gunson, Ref. 2, and D. I. Olive, Nuovo Cimento 29, 326 (1963).

24. This argument is taken from Ref. 3.

25. Details are given in Appendix E.

26. This is essentially the result of Ref. 7.

27. This is essentially the result of Ref. 8.

28. This topic will be discussed in more detail in later work.

29. The application of Fredholm theory to the problem of continuation of many-particle scattering amplitudes to unphysical sheets has been discussed earlier by H. P. Stapp, Lawrence Radiation Laboratory Report UCRL-10261 (1962) and Nuovo Cimento 32, 103 (1964); J. Gunson (Ref. 2); and D. I. Olive, Nuovo Cimento 28, 1318 (1962).

30. D. I. Olive, Phys. Rev. 135, B745 (1964); see also R. J. Eden,

P. V. Landshoff, D. I. Olive, and J. C. Polkinghorne, The Analytic S-Matrix (Cambridge University Press, Cambridge, 1966), p. 212.

31. The argument is essentially the same as in the proof of the Third Structure Theorem of Ref. 13.

32. A. Martin, CERN preprint.

33. J. B. Boyling, Nuovo Cimento 33, 1356 (1964).

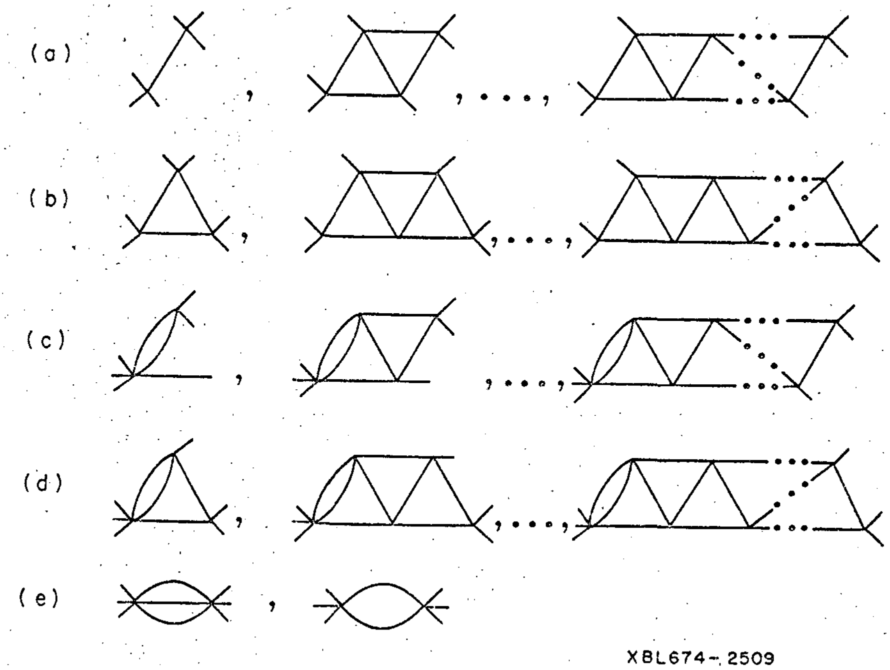

Fig. 1. The elementary diagrams of the $3 \to 3$ amplitude below the four-particle threshold. All positive-α Landau surfaces for the $3 \to 3$ amplitude below the four-particle threshold are contained in the union of the positive-α Landau surfaces corresponding to the set of diagrams consisting of (1) the set of elementary diagrams; (2) the set of reflections of elementary diagrams; and (3) the set of diagrams obtained from diagrams of these two sets by replacing any set of simple inner vertices by single two-particle closed loops. Simple vertices are vertices directly connected to no other vertex by more than one line. Inner vertices are vertices not standing on the extreme right or left of the diagram. The second figure in (e) contains a single two-particle closed loop. The analogous part of the first figure in (e) is called a three-particle closed loop.

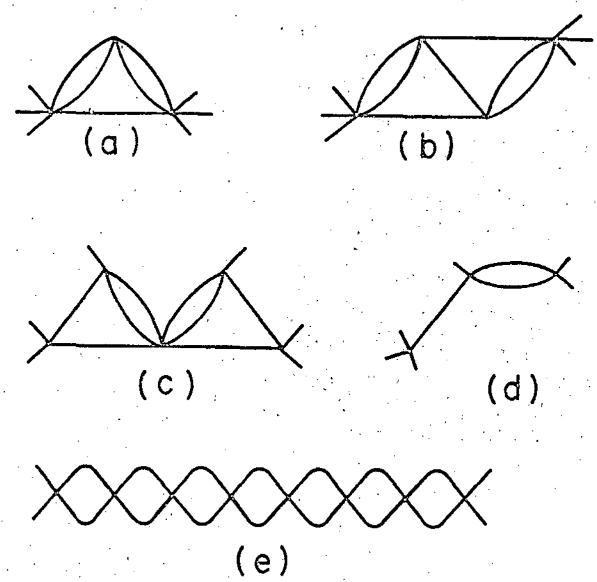

XBL674-2510

Fig. 2. Various Landau diagrams corresponding to Landau surfaces contained in the Landau surfaces of the diagrams described in Fig. 1. A diagram containing more than one $2 \to 3$, $3 \to 2$, or $3 \to 3$ vertex, such as one of the above diagrams (a) and (b), corresponds to a Landau surface that is confined to the surface corresponding to one of the diagrams (e) of Fig. 1. The diagrams (c) and (d) contain two "independent parts" that are diagrams described in Fig. 1. The Landau surfaces of the full diagrams are confined to the intersections of the Landau surfaces corresponding to their independent parts. The Landau surface corresponding to the chain of two-particle closed loops (e) is confined to the Landau surface corresponding to the single two-particle closed loop in (e) of Fig. 1.

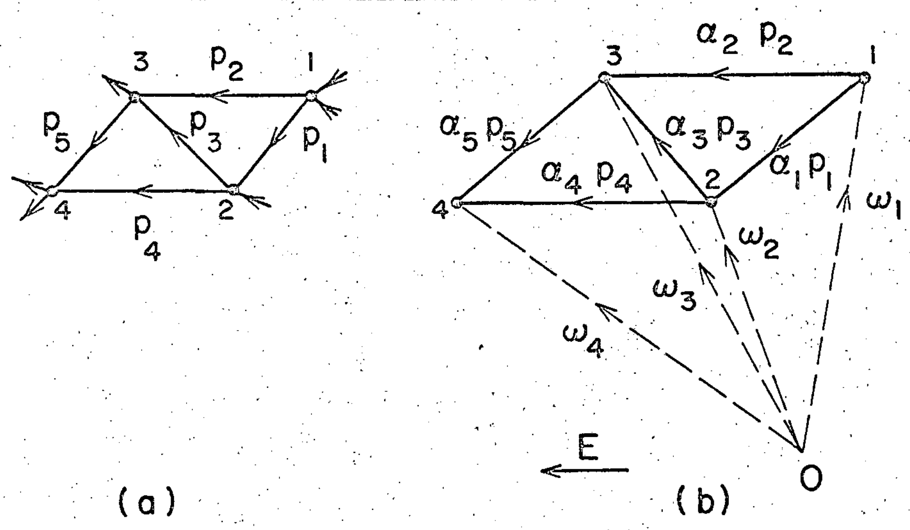

XBL674-2523

Fig. 3. Figure (a) shows a diagram D, and Fig. (b) shows a corresponding $\bar{D}$ with all α's positive. In diagram (b) positive energy vectors point left. The condition that all α's be positive, together with the energy-conservation law, ensures that the diagram $\bar{D}$ has the "physical" ordering, with energy flowing into the right-most vertex V_1 and out of the left-most vertex V_n. If the signs of the α's are all reversed, then the relative positions of the vertices of the new $\bar{D}$ are obtained by reflecting diagram (b) through the origin O.

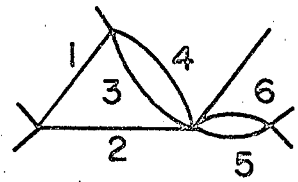

XBL674-2532

Fig. 4. An example of a Landau diagram containing a vertex V through which must pass every path connecting any initial line to any final line. A path connecting lines is required to connect internal points of these lines.

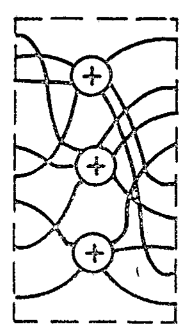

XBL674-2595

Fig. 5. Diagram representing a typical term M_p of the M function in (A.1a).